

Final Technical Report

Submitted to

National Aeronautics and Space Administration

Grant # NAG 5-2585

**Field Micrometeorological Measurements, Process-Level Studies
and Modeling of Methane and Carbon Dioxide Fluxes
in a Boreal Wetland Ecosystem**

PRINCIPAL INVESTIGATOR

University of Nebraska-Lincoln

S. B. Verma, Professor, School of Natural Resource Sciences and Director, Center for Laser-Analytical Studies of Trace Gas Dynamics; PHONE: (402) 472-6702 or 472-3679; FAX: (402) 472-6614. E-Mail: agme009@unlvm.unl.edu

CO-PRINCIPAL INVESTIGATORS

University of Nebraska-Lincoln, (UNL)

T. J. Arkebauer, Associate Professor,
Department of Agronomy

F. G. Ullman, Professor Emeritus
Department of Electrical Engineering
and Center for Laser-Analytical Studies
Trace Gas Dynamics.

Colorado State University (CSU) and National Center for Atmospheric Research (NCAR)

D. W. Valentine, Research Associate
Natural Resource Ecology
Laboratory, CSU (Now Assistant
Professor, Department of Forest
Sciences, University of Alaska,
Fairbanks, AK)

W. J. Parton, Professor, Department
of Range Science, CSU

D. S. Schimel, Scientist III, NCAR;
Research Scientist, NREL; and
Adjunct Associate Professor,
Department of Forest Sciences, CSU

TABLE OF CONTENTS

	Page
SUMMARY	
1. Project Objectives	1
2. Study Site and Vegetation	1
3. Brief Description of Research and Primary Results	4
3.1 Micrometeorological Measurements of Fluxes of Carbon Dioxide and Methane	4
3.1.1 Overall Micrometeorological Setup	4
3.1.2 Carbon Dioxide Flux	5
3.1.3 Methane Flux	11
3.2 Chamber Measurements of Surface Carbon Dioxide Flux	16
3.3 Chamber Measurements of Individual Leaf Gas Exchange	20
3.4 Chamber Methane Flux and Associated Measurements	24
4. Scientific Publications Stemming from this Project	27
4.1 Journal Articles	27
4.2 Papers Presented	28
5. References	30
6. Tables and Figures	33

1. PROJECT OBJECTIVES

The primary objectives of this grant, as part of BOREAS (Boreal Ecosystem-Atmosphere Study), are to:

- 1) Quantify, employing the micrometeorological eddy correlation technique, the surface exchange rates of methane and carbon dioxide at a boreal wetland site.
- 2) Evaluate the soil surface carbon dioxide flux and characterize its response to controlling variables (such as temperature, water content, water table depth).
- 3) Conduct process-level studies (field experimental manipulations) to quantify the degree of substrate quantity and quality limitations on methane production, oxidation and emission. Quantify the responses of leaf photosynthesis, plant respiration and stomatal conductance of dominant plant species to relevant controlling variables.
- 4) Integrate the first three components to test and improve a model of decomposition and methane emission responsive to variability in moisture, temperature and plant productivity in northern wetland ecosystems. (This effort has been substantially reduced due to the budget reduction, and may be undertaken using other resources.)

2. STUDY SITE AND VEGETATION

Our research site (the BOREAS SSA Fen Site) is a patterned fen surrounded by black spruce and jack pine forests. Patterned fens are characterized by alternating strings (higher, usually drier areas) and flarks (lower, usually wetter areas) which are oriented perpendicular to the hydrologic flow. The main hydrologic flow in the SSA Fen is from north to south; in places a distinct channel of flowing water becomes visible between small pools. The fen is approximately 500 m wide (east-west) and 2 km long (north-south). The micrometeorological flux tower is located in the southern

part of the fen. The tower location has reasonable fetch from the north, west and south (180⁰-360⁰). Strings are relatively uncommon, or poorly developed, in this area. The depth of the peat soil is 2-3 m in the center of the fen and 1 m near the edges. The peat surface is not flat; it consists of small hummocks (microhills) and small hollows (microvalleys).

On July 31, 1993 we established two transects from east to west across the fen in the vicinity of the main tower location. Every six meters we identified the plants nearest the transect and noted whether the surface was covered with standing water or not. Out of the 122 total transect locations sampled 59 (48%) had standing water. However, the fen drains fairly rapidly and the water table fluctuates in response to drainage and local precipitation. Therefore, the amount of the fen exposed to the atmosphere also changes from day to day; this has implications for the spatially-averaged soil surface CO₂ flux (see Section 3.2).

Dominant woody plant species are 1-1.5 m tall bog birch (*Betula pumila*) and, on the strings, 2-4 m tall tamarack (*Larix laricina*). Buckbean (*Menyanthes trifoliata*) and several sedges (*Carex* spp.) are abundant herbaceous species throughout the fen. Most hummocks consist of live and dead *Carex* spp., some are dominated by green mosses (e.g., *Tomenthypnum nitans*, *Hylacomium splendans*). Several species of brown moss (e.g., *Calliergon* sp., *Drapanocladus* sp.) are common in the wetter hollows. Other common vascular plants include horsetail (*Equisetum fluviatile*), marsh cinquefoil (*Potentilla palustris*), marsh marigold (*Caltha palustre*), bog rosemary (*Andromeda polifolia*) and several willows (*Salix* spp.).

In 1995 we determined the seasonal course of leaf area index (LAI) for areas of the fen which were representative of the tower footprint. On seven days spanning the 1995 growing season, twenty 0.25 m² plots were harvested. The vegetation was clipped and separated by species for each

plot. Total green leaf areas and dry weights were determined for each species on each sampling date.

The total green LAI was 0.1 in late May, it peaked near 1.3 in late July, and decreased to 0.1 by late September (Fig. 1). After June 1st, over 70% of the total LAI consisted of foliage from *Betula pumila*, *Menyanthes trifoliata* and *Carex* spp. Of the remainder, about 15% consisted of foliage from various *Salix* species. The different plant species had different seasonal patterns of leaf area development. For example, *Carex* emerged earliest, while *Menyanthes* emerged latest.

The mid-season peak in total green LAI in 1995 was quite similar to a 1994 value (LAI = 1.2 on July 25, 1994) determined by J. Chen as part of the BOREAS core measurement program.

3. BRIEF DESCRIPTION OF RESEARCH AND PRIMARY RESULTS

3.1 MICROMETEOROLOGICAL MEASUREMENTS OF FLUXES OF CARBON DIOXIDE AND METHANE

3.1.1 Overall Micrometeorological Setup

The main instrumentation platform consisted of eddy correlation sensors mounted on a scaffold tower at a height of 4.2 m above the peat surface. The sensors were attached to a boom assembly which could be rotated into the prevailing winds. The boom assembly was mounted on a movable sled which, when extended, allowed sensors to be up to 2 m away from the scaffolding structure to minimize flow distortion. When retracted, the sensors could easily be installed, serviced or rotated. An electronic level with linear actuators allowed the sensors to be remotely levelled once the sled was extended.

Two instrument arrays were installed. A primary (fast-response) array consisted of a three-dimensional sonic anemometer, a methane sensor (tunable diode laser spectrometer), a carbon dioxide/water vapor sensor, a fine wire thermocouple and a backup one-dimensional sonic anemometer. The secondary array consisted of a one-dimensional sonic anemometer, a fine wire thermocouple and a Krypton hygrometer. Descriptions of these sensors may be found in other reports (*e.g.*, Verma, 1990; Suyker and Verma, 1993).

Slow-response sensors provided supporting measurements including mean air temperature and humidity, mean horizontal windspeed and direction, incoming and reflected solar radiation, net radiation, incoming and reflected photosynthetically active radiation (PAR), soil heat flux, peat temperature, water-table elevation and precipitation. A data acquisition system (consisting of an IBM compatible microcomputer, amplifiers and a 16 bit analog-to-digital converter), housed in a small trailer, was used to record the fast response signals. These signals were low-pass filtered (using 8-pole Butterworth active filters with a 12.5 Hz cutoff frequency) and sampled at 25 Hz.

Slow-response signals were sampled every 5s using a network of CR21X (Campbell Scientific, Inc., Logan Utah) data loggers installed in the fen. All signals were averaged over 30-minute periods (runs).

3.1.2 Carbon Dioxide Flux

Seasonal Distributions of Atmospheric CO₂ Flux

Seasonal distributions of the midday (1130 - 1430 hrs, CST) atmospheric CO₂ flux (or net ecosystem exchange, F_c in $\text{mg CO}_2 \text{ m}^{-2} \text{ (ground area) s}^{-1}$) during the 1994 and 1995 growing seasons are presented in Fig. 2 (flux toward the surface is positive). Generally, F_c was comparable in pattern and magnitude in the two seasons. In the beginning of the season (May 19-20: DOY 139-40) in both years, the CO₂ flux was slightly less than zero. The flux became positive by May 28 (DOY 148) and began to increase rapidly reaching about $0.15 \text{ mg m}^{-2} \text{ s}^{-1}$ by May 31 (DOY 151) in both years. By the end of June in both years, F_c increased to $0.4 \text{ mg m}^{-2} \text{ s}^{-1}$. The rapid rise in F_c corresponded to the increase in leaf area index (LAI) during the same period (Fig. 1). The seasonal peak of F_c was about $0.50\text{-}0.60 \text{ mg m}^{-2} \text{ s}^{-1}$ and occurred in the first week of July in both years. This peak coincided with the seasonal maximum in LAI. Following the peak, the flux decreased in magnitude to $0.35 \text{ mg m}^{-2} \text{ s}^{-1}$ by the first week of August (DOY 219) in both years. The LAI also decreased similarly. For the remainder of August and during September as the vegetation senesced, F_c declined gradually dropping below zero near the end of September (DOY 270).

There were some periods when the magnitude of F_c in 1995 was larger than 1994. During the three day period of June 21-23 (DOY 172-174) in 1995, F_c was up to $0.49 \text{ mg m}^{-2} \text{ s}^{-1}$, about double the flux of 0.19 to $0.29 \text{ mg m}^{-2} \text{ s}^{-1}$ during the same period in 1994. Incident PAR was not limiting (Fig. 3). Water table was similar in height during this period in both years (Fig. 4).

Reduced CO₂ flux in this period in 1994 seems to be associated with high vapor pressure deficit (D) and air temperature (T) (midday D \approx 1.9 - 2.8 kPa in 1994 and 0.6 - 1.0 kPa in 1995; midday T \approx 24-30°C in 1994 and 15-18°C in 1995: Fig. 3).

During July 20-August 2 (DOY 201-214) in 1995, F_c was 0.45 mg m⁻² s⁻¹, compared to 0.25 mg m⁻² s⁻¹ during the same period in 1994. Incident PAR was not limiting (except for July 30: DOY 211). Again, the reduced CO₂ flux in this period in 1994 seems to be associated with high vapor pressure deficit and air temperature (midday D \approx 1.2 - 2.4 kPa in 1994 and 0.3 - 0.8 kPa in 1995; midday T \approx 21 - 30 °C in 1994 and 12 - 20 °C in 1995: Fig. 3). Also, on the night of July 18/19 (DOY 199/200) in 1994, a heavy rainfall caused the water table to rise from 0.21 to 0.30 m (Fig. 4). The large sudden increase in W was estimated to have inundated about 25% of the canopy LAI. This may have contributed to the smaller flux during this period in 1994.

Environmental Controls

a) Daytime Atmospheric CO₂ Flux

Light response of atmospheric CO₂ flux (half-hourly data) for moderate vapor pressure deficit (0.0 < D < 1.5 kPa) and air temperature (5 < T < 20 °C) during midseason of 1994 and 1995 is shown in Fig. 5A. A rectangular hyperbola of the form;

$$F_{cL} = f(\text{PAR}) = \alpha \text{ PAR } F_{cL\infty} / (\alpha \text{ PAR} + F_{cL\infty}) - R_{sL} \quad (1)$$

was fit to the data where F_{cL} ($= F_c/\text{LAI}$) is the atmospheric CO₂ flux (mg m⁻² (leaf area) s⁻¹), α is the slope of the curve at $F_{cL} = 0$, $F_{cL\infty}$ is the atmospheric CO₂ flux (mg m⁻² (leaf area) s⁻¹) asymptote and R_{sL} is the dark respiration. The values and confidence intervals of α , $F_{cL\infty}$, and R_{sL} are given in Table 1. In general, the CO₂ flux-PAR relationship for the two seasons seem to be quite similar.

The data suggest that the canopy approaches light saturation for PAR above 1000 - 1200 $\mu\text{mol m}^{-2} \text{s}^{-1}$ in both seasons.

For moderate conditions in both years, the model fit the data quite well ($r^2 \approx 0.75$). The CO_2 flux-PAR relationship for moderate D and T in both years are statistically identical since the 95% confidence intervals overlap for each model parameter. Model parameters in Table 1 were compared to those from a similar analysis done by Frohking *et al.* (1998) for rich fens in central Manitoba (BOREAS northern study area) and the Hudson Bay lowlands (note our study uses F_c normalized by LAI, but during midseason LAI was near one and so comparisons are reasonable).

Values of α ranged from 0.0004 to 0.0011 $\text{mg m}^{-2} \text{s}^{-1}/\mu\text{mol m}^{-2} \text{s}^{-1}$ in their study compared to 0.0009 to 0.0013 $\text{mg m}^{-2} \text{s}^{-1}/\mu\text{mol m}^{-2} \text{s}^{-1}$ here. Their asymptote $F_{cL\infty}$ ranged from 0.18 to 0.66 $\text{mg m}^{-2} \text{s}^{-1}$ compared to 0.44 to 0.69 $\text{mg m}^{-2} \text{s}^{-1}$ in our study. Also R_{sL} ranged from 0.07 to 0.15 $\text{mg m}^{-2} \text{s}^{-1}$ which was comparable to 0.13 to 0.20 $\text{mg m}^{-2} \text{s}^{-1}$ in our study.

As indicated in Fig. 5B, the CO_2 flux distinctly decreases under high vapor pressure deficit and temperature conditions (*i.e.*, $2.0 < D < 3.2 \text{ kPa}$ and $20 < T < 30 \text{ }^\circ\text{C}$). The F_c -PAR relationship (Eq. 1) suggests that under these conditions, $F_{cL\infty}$ was approximately 36% smaller and dark respiration (R_{sL}) was 43% larger (Table 1), compared to moderate conditions (the lower r^2 under high D and T conditions could be due to the lack of data at low light levels). The high vapor pressure deficit and temperature conditions likely induced stomatal closure and increased respiration, consequently reducing the net carbon uptake. This conclusion is supported by results from our chamber measurements of individual leaf gas exchange (see Sec. 3.3). In those studies, on a leaf area basis, dark respiration rates were exponentially related to leaf temperature with a Q_{10} near two (Fig. 15) and stomatal conductances decreased 50% as vapor pressure deficits increased from 1.0 to 3.5 kPa.

Fig. 6 is an empirical attempt to examine the effect of high D on atmospheric CO₂ flux (as indicated earlier, high D values were generally associated with high T). In this figure, midday values of $F_{cL}/f(\text{PAR}) = g(D)$ are plotted against D, where $f(\text{PAR})$ is the light dependence of CO₂ flux for moderate vapor pressure and temperature conditions in 1995 (Eq. 1). Effect of high values of D is clearly seen for $D > 1.5$ kPa. The value of $g(D) = F_{cL}/f(\text{PAR})$ was nearly 1.0 for $D \leq 1.5$ kPa and began to decrease for $D > 1.5$ kPa, reaching to a value of about 0.5 at $D = 3.0$ kPa. Frolking *et al.* (1996) modeled a similar relationship for a boreal spruce canopy. Their magnitude of $g(D)$ was about 0.8-0.9 when D was equal to 1.5 kPa and decreased to about 0.5 for D at 3 kPa.

The empirical relationship discussed above allows us to examine the overall consistency of the CO₂ flux data in the two seasons. To do this we used the 1995 light response (F_c -PAR) relationship for moderate conditions and a linear adjustment for high vapor pressure deficit ($D > 1.5$ kPa: Fig. 6) to the measurements of PAR, T and D during the midseason in 1994. For the period with the sudden rise in water table (July 20-26, DOY 201-207, 1994), we also incorporated a reduction in CO₂ flux based on our estimate that about 25% of the leaf area was inundated. Empirically estimated F_c compares reasonably well with the measured fluxes, suggesting good consistency between the two seasons of flux measurements (Fig. 7).

b) Nocturnal Atmospheric CO₂ Flux

Results on averaged nighttime (2200-0400 hrs, CST) CO₂ flux are presented in Fig. 8 (nocturnal flux measurements become less reliable under low windspeed conditions and so data for $u_* > 0.15 \text{ m s}^{-1}$ are considered here). The magnitude of average nighttime flux ranged from 0.04 to 0.11 $\text{mg m}^{-2} \text{ s}^{-1}$ in 1994 and 0.03 to 0.20 $\text{mg m}^{-2} \text{ s}^{-1}$ in 1995. Average nighttime peat temperatures ranged from 4.8 to 21.1°C in 1994 and 3.3 to 17.4°C in 1995.

As observed in other studies (*e.g.*, Bubier *et al.*, 1995), changes in peat temperature seem to track changes in the water table height (Figs. 4A and B): the higher peat temperatures in 1994 corresponded to periods of higher water table. The nocturnal flux was small in both seasons when the peat temperature was below about 10°C. In 1995 when the peat temperature became greater than 12°C, the flux increased rapidly to 0.20 mg m⁻² s⁻¹ when the peat temperature reached 17°C. In 1994, however, the flux magnitude remained less than 0.11 mg m⁻² s⁻¹ when the peat temperature ranged between 12 and 21°C. We believe that the difference in the nighttime CO₂ flux between the two seasons is likely due to the higher water table in 1994. This observation is consistent with previous studies (*e.g.*, Whiting, 1994; Moore and Dalva, 1993; Freeman *et al.*, 1993; Funk *et al.*, 1994; Oberbauer *et al.*, 1992; Oechel and Billings, 1992; Billings *et al.*, 1982; 1983) which indicate a decrease in CO₂ emission from the peat with increasing water table heights. It is also consistent with our results from chamber measurement of surface CO₂ flux (see Sec. 3.2). For example, results shown in Fig. 13 indicated that, at constant temperature, the surface CO₂ flux decreases as the water table height increases.

Integrated Net Ecosystem CO₂ Exchange

Half-hourly values of the atmospheric CO₂ flux measured during May 20 to October 6 in 1994 and 1995 were integrated to calculate the daily net ecosystem exchange. To fill in the missing half-hourly data for brief periods (due to unacceptable wind direction, sensor malfunction and calibration periods), we used a combination of interpolation and empirical data synthesis (*e.g.*, Baldocchi *et al.*, 1997). Interpolation was used during periods of relatively constant environmental conditions. In empirical data synthesis, atmospheric CO₂ flux was estimated as a function of PAR, D and T during the day (Eq. 1 and Fig. 5). At night, flux was estimated as a function of peat

temperature (Fig. 8). In 1995, for extended periods of missing flux data in early June and late August, NEE was estimated as follows. First, a rectangular hyperbolic relationship between daily NEE and the daily sum of incident solar radiation (similar to Eq. 1) was established using a few days of data soon after measurements resumed. This relationship was used to estimate NEE during the missing period after adjusting the asymptotic NEE as a linear function of LAI. The daily sum of incident solar radiation at our site was estimated from an established relationship (slope = 0.98, $r^2 = 0.72$) between daily integrated sums of incident solar radiation measured at our site and the Old Aspen site (located 105 km to the southwest of our site - *e.g.*, Sellers *et al.*, 1995).

Information on cumulative NEE for the two seasons is given in Fig. 9. Early in the season until June 6 (DOY 157), there was virtually no difference between cumulative NEE (in 1994 and 1995. Then by June 24 (DOY 175) the cumulative NEE was 23 g C m⁻² in 1995 and near zero in 1994. In 1994 the period June 6-24 had many days with near- zero NEE because of high daytime air temperature and vapor pressure deficit. As discussed earlier, the days June 21-23 (DOY 172-174), in particular, had F_c in 1994 only half the magnitude in 1995. Cumulative NEE was 79 and 120 g C m⁻² on August 3 (DOY 215) in 1994 and 1995, respectively — the largest difference (41 g C m⁻²) between the two seasons. July 20 - August 2 (DOY 201-214) in 1994 was another period of high daytime air temperature and vapor pressure. In 1995, the first two weeks in August (DOY 215-225) had many overcast days which decreased the difference in cumulative NEE from 41 to about 30 g C m⁻². At the end of the measurement period the integrated NEE was calculated to be 88 and 121 g C m⁻² for the growing seasons of 1994 and 1995, respectively.

In a peatland in central Minnesota (peak LAI \approx 0.6), Shurpali *et al.* (1995) measured a net carbon uptake of 32 g C m⁻² over a growing season with moderate water table conditions (a net carbon loss of 71 g C m⁻² was measured in a previous growing season which was relatively dry).

In the Hudson Bay lowlands, Whiting (1994) measured a net uptake of 6 g C m^{-2} to a net loss of 21 g C m^{-2} in wetlands with LAI generally between 0.2 to 0.5 (up to 1.1 at one site). The larger carbon uptake at our site is consistent with the high productivity (peak LAI ≈ 1.3) and large methane efflux (Suyker *et al.*, 1997). In a Finnish oligotrophic pine fen, Alm *et al.* (1997) estimated net carbon uptake (using transparent chambers) of 44 g C m^{-2} over the growing season. Studies in boreal forests in Quebec (black spruce forest: Fan *et al.*, 1995) and near our wetland site (black spruce forest: Jarvis *et al.*, 1995; jack pine forest: Baldocchi *et al.*, 1997) have reported net carbon uptake of comparable magnitude ($47\text{-}180 \text{ g C m}^{-2}$). None of these studies included winter respiratory losses so annual NEE may be smaller (*e.g.*, Mosier *et al.*, 1993).

3.1.3 Methane Flux

Seasonal Distributions of Methane Flux

Seasonal patterns of midday (1130-1430 hrs, CST) methane flux (F_m in $\text{mg CH}_4 \text{ m}^{-2}(\text{ground area}) \text{ s}^{-1}$) measured during the 1994 and 1995 growing seasons are presented in Fig. 10. In 1994, F_m gradually increased from near zero to about $0.5 \text{ mg m}^{-2} \text{ h}^{-1}$ from May 19-June 1 (DOY 139-152). Then, during the first three weeks in June of 1994, F_m continued to increase steadily reaching $2.0 \text{ mg m}^{-2} \text{ h}^{-1}$ by June 20 (DOY 171). In the early part of the season (\approx May 19 to June 1; DOY 139-152) in 1995, however, F_m was larger: during this period, the flux increased from 0.7 to $3.0 \text{ mg m}^{-2} \text{ h}^{-1}$.

On June 1, 1995 (DOY 152), we were forced to remove our equipment due to a rapidly approaching forest fire approximately 40 km north of the site. Flux measurements resumed on June 20, 1995 (DOY 171) and F_m was $16.4 \text{ mg m}^{-2} \text{ h}^{-1}$. On the following day (June 22, 1995: DOY 173) F_m was $16.5 \text{ mg m}^{-2} \text{ h}^{-1}$, the largest methane flux measured in 1995 (unfortunately, because

of the gap in data collection, it is difficult to suggest the exact time and magnitude of the peak flux in 1995). In comparison, F_m in 1994 continued a relatively gradual increase from June 1 (DOY 152) until about mid July reaching $6.2 \text{ mg m}^{-2} \text{ h}^{-1}$ on July 16 (DOY 197). Following a series of heavy rains in mid to late July, F_m began to increase rapidly. The flux increased from 6.2 to $19.5 \text{ mg m}^{-2} \text{ h}^{-1}$ in a 16 day period with a seasonal peak of $19.5 \text{ mg m}^{-2} \text{ h}^{-1}$, occurring on August 1 (DOY 213) in 1994. Thus, the largest methane flux in 1995 occurred about $5\frac{1}{2}$ weeks before the peak flux measured in 1994. In each year following the seasonal peak, F_m decreased uniformly to 1.5 and $2.8 \text{ mg m}^{-2} \text{ h}^{-1}$ around October 8 (DOY 281) in 1995 and 1994, respectively.

The seasonal patterns of water table (W : above an average hollow surface) and peat temperature (T_p : 10 cm below an average hollow surface) also showed contrasting patterns between the two years (Fig. 4A and B). In the early part of the growing season (\approx DOY 140), W was 9 cm in 1994 compared with 20 cm in 1995. However, after a series of rains in late May in 1994, W was 17 cm by June 1 (DOY 152) compared with 18 cm on this day in 1995. When measurements resumed on June 20-22 (DOY 171) in 1995, W was 15 cm comparable to the value 18 cm at this time in 1994. Water table in 1995 followed a generally decreasing trend for the rest of the season in 1995. The value of W was fairly low (5-7 cm) during the last week of July and first week of August (DOY 220). In contrast to 1995, W in 1994 increased rapidly in early July (DOY 184) from 16 cm to its maximum 30 cm on July 20 (DOY 201). Following the seasonal peak, W showed a steady decrease to about 8 cm in early October 1994. Peat temperature in both seasons showed similar trends until June 1 (DOY 152). Temperatures generally increased from 2 to 9°C in 1995. By June 20 (DOY 171) in 1995, T_p was 17°C , its the seasonal peak. In contrast, peat temperature in 1994 on this day was 12°C . During July, T_p increased similar to W reaching the seasonal peak

of 19°C on August 1 (DOY 213). By early October (\approx DOY 279) in both seasons, peat temperature generally decreased to about 4-6°C.

The seasonal distributions of methane flux, water table, and peat temperature in the two seasons exhibited many similarities and some differences. In both growing seasons, F_m showed a period of rapid increase to reach the seasonal peak: a change of 13.5 mg m⁻² h⁻¹ in a 21-day period in 1995 and a 13.3 mg m⁻² h⁻¹ change in flux during a 16-day period in 1994. Also, the magnitude of peak methane flux was comparable in both seasons: 16.5 and 19.5 mg m⁻² h⁻¹ in 1995 and 1994, respectively. The highest peat temperature were similar (17°C in 1995 and 19°C in 1994) and occurred at about the same time as the peak methane flux. Water table was also high (>15 cm) during peak F_m and T_p .

In contrast, the peaks in methane flux and peat temperature occurred about 5 to 6 weeks earlier in 1995 compared to 1994. In the early part of the 1995 season, there was a relatively rapid increase in methane emissions. High water table during this period may have enhanced methane production, as the peat warmed and methanogen community became active. In 1994, however, the onset of methane production in May/June remained gradual and the rapid increase in F_m didn't occur until after the water table had become much higher. In 1994 the highest water table was on July 20 (DOY 221) and preceded the peak methane flux on August 1 by about 12 days. A lag between changes in water table and methane flux has been observed in other studies (Dise *et al.*, 1993; Moore and Dalva, 1993). However, evidence of a lag in 1995 was not so clear since the water table was already high when methane flux increased in June. In general, seasonal patterns of methane flux, peat temperature and water table were similar in a given growing season, but very different when compared to the other season.

Chamber measurements of methane flux during two consecutive growing seasons in a New Hampshire fen by Frolking and Crill (1994) show similar patterns of methane flux as observed in our study. The first season was comparable to 1995. Spring was relatively warm and moisture levels were near normal. Parallel to the seasonal pattern of F_m in this study, peak methane flux occurred late June/early July. The methanogenic community seemed to have had an early and vigorous start and there was a rapid increase in methane flux to the seasonal peak (heavy rains from a hurricane caused flooding in the fen that may have reduced the methanogen community or anaerobic conditions, suppressing F_m later in the season). In their next season (similar to 1994 in our study), spring was drier and there was a more gradual increase to the peak flux which occurred in August. They observed a difference of about 4 weeks between seasonal peak CH_4 fluxes between the two growing seasons.

Integrated Methane Flux

Measured methane flux was integrated to estimate net methane emission during the two growing seasons. Based on the observed diurnal patterns, the flux was assumed to be approximately constant during the day and during the night. Data for missing daytime periods were filled in by using the regression relationships (methane flux as a function of peat temperature and water table) derived from measurements in this study. Data for missing nighttime periods were filled in by adjusting daytime flux with the ratio of daytime/night flux observed on the nearest day.

The fen emitted $16.3 \text{ g C-CH}_4 \text{ m}^{-2}$ in the 1994 growing season and $18.1 \text{ g C-CH}_4 \text{ m}^{-2}$ in the 1995 growing season. The magnitude of integrated methane flux was similar between the two seasons, as were the seasonal peak magnitudes of methane flux, water table and peat temperature but, as discussed above, these peaks occurred at different times. In southern and middle boreal

peatlands in Finland, over a period of two years, Nykanen *et al.* (1996) measured integrated methane flux generally ranging from 15-32 (up to 54 at one site) g C-CH₄ m⁻² in undrained fens (fluxes were integrated over a year in that study but methane emission during winter months would be quite small, so a comparison with the growing season-integrated methane flux of this study is reasonable). They also noted higher methane fluxes between years corresponded to warmer seasons with a high water table. In eastern Finland, Saarino *et al.* (1996) measured methane emission in a sedge/pine fen complex of hummock, lawn, and flark microsites of 20.2 g C-CH₄ m⁻² during a period similar to this study. In a North American fen in New Hampshire (43°N), Frohling and Crill (1994) measured an annual methane release of 52 g C-CH₄ m⁻² each year in 1991 and 1992. In peatlands of Minnesota, Dise *et al.* (1993) and Crill *et al.* (1992) have reported (yearly) integrated methane emission from 3.4 to 70 g C-CH₄ m⁻². Shurpali and Verma (1998) measured methane emission of 10.4 and 11.5 g C-CH₄ m⁻² over two consecutive 5-month growing seasons also in a Minnesota peatland (1991 and 1992, respectively). In the Canadian Hudson Bay lowlands and northern Ontario, however, Roulet *et al.* (1994) and Bubier *et al.* (1993) have reported lower annual CH₄ emissions of 0.2-14 g C-CH₄ m⁻² and 3.4 g C-CH₄ m⁻², respectively.

The carbon released in methane emission during the growing season was 19% of the net ecosystem exchange of CO₂ observed in a concurrent study (Suyker *et al.*, 1996 and 1997) in 1994 (16.3 g C-CH₄ m⁻² and 88 g C-CO₂ m⁻²) and 15% in 1995 (18.1 g C-CH₄ m⁻² and 121 g C-CO₂ m⁻²). Shurpali *et al.* (1993) measured 33% of the net ecosystem CO₂ uptake was released as methane in a Minnesota peatland (LAI ≈ 0.6) during a wet growing season in 1992 (10.4 g C-CH₄ m⁻² and 32 g C-CO₂ m⁻²). In a sedge/pine fen in Finland, Alm *et al.* (1997) found that the carbon released from methane was 32% of the net ecosystem CO₂ exchange (22 g C-CH₄ m⁻² and 68 g

C-CO₂ m⁻²) over a year. These studies demonstrate that, in general, carbon loss from methane emission in northern wetlands can be an important part of the carbon budget.

3.2 CHAMBER MEASUREMENTS OF SURFACE CARBON DIOXIDE FLUX

The surface of the fen is heterogenous. Areas of open water alternate with 2-20 cm tall hummocks composed of more or less consolidated dead vegetation. Larger features include strings, where the peat surface is ca. 20-50 cm above the water table, and flarks, which are more extensive areas of open water. These features are associated with different surface CO₂ (and CH₄) fluxes. We measured surface CO₂ fluxes using a portable, closed-loop gas exchange system (LI-6200, Li-Cor, Inc., Lincoln NE) connected to a one liter cylindrical stainless steel measurement chamber that covered approximately 83 cm² of the fen surface. For the 1993 pilot study, a different measurement chamber was used which also had a one liter volume but only covered about 43 cm² of the surface. The gas exchange system was used in a closed-loop configuration. During the measurements the chamber was sealed against PVC collars which had previously been sunken into the surface of the fen. A tripod was used to hold the chamber steady. The CO₂ concentration in the chamber was drawn down ca. 20 ppm below ambient and allowed to rise (due to the surface flux). Data were logged as the chamber CO₂ concentration increased through the ambient concentration. At each collar location, soil temperature at 10 cm below the surface was logged during the measurement. The distance from the surface to the water table was determined immediately after the flux measurement. Fluxes were determined from the change in chamber CO₂ concentration during a measurement interval. Individual flux determinations took about one minute to complete. In addition to the CO₂ concentration, the system recorded the temperature and relative humidity of the air above the surface and a near surface (0.1 m deep) peat temperature.

A pilot study was conducted during August and September, 1993. At the beginning of August, 20 PVC collars were placed near the main boardwalk. Half of these were in open water and the other half were on top of hummocks. Measurements of surface CO₂ flux were made on these collars from 2-8 August 1993.

In mid-August two permanent boardwalks were laid out (one north and one south of the main boardwalk) and six platforms were erected on each boardwalk. Half of the platforms were located on obvious strings. Four PVC collars were placed at each platform such that two were in open water and two were on either hummocks or on the tops of strings. These 48 collars were used for surface CO₂ flux measurements from 21 August, 1993 to 7 September, 1993.

Collars associated with platforms considered to be representative of the micrometeorological tower footprint were all located in extensive areas of *Betula pumila*. The surface consisted of sedge hummocks interspersed with open water where *Menyanthes trifoliata* was common. The total surface area near these locations was approximately equally divided between hummocks and open water. Mean surface fluxes from these locations in 1993 ranged from -0.060 mg CO₂ m⁻² s⁻¹ to -.096 mg CO₂ m⁻² s⁻¹. As is commonly found for these types of measurements, the variability was fairly high.

The distance between the surface enclosed by the PVC collars and the water surface ranged from 0-25 cm. These distances were not constant for a given collar due to precipitation patterns during the five week measurement period.

Our results from the pilot study indicated that, in general, surface CO₂ fluxes increased with increasing distance above the water surface and surface CO₂ fluxes increased with increasing peat temperature. In addition, fluxes from open water surfaces were smaller than those from hummocks,

although as the hummocks dried out, their fluxes decreased until there was little difference between the two locations.

Surface fluxes were measured from late May through September, 1994 at the twelve 1993 platform locations. The seasonal patterns of surface fluxes are shown in Fig. 11. Fluxes were small early in the season (*e.g.*, $-0.05 \text{ mg CO}_2 \text{ m}^{-2} \text{ s}^{-1}$ on May 27, DOY 147). Midseason values averaged about $-0.10 \text{ mg CO}_2 \text{ m}^{-2} \text{ s}^{-1}$ with occasional fluxes near $-0.2 \text{ mg CO}_2 \text{ m}^{-2} \text{ s}^{-1}$. By late September these values had decreased to about $-0.05 \text{ mg CO}_2 \text{ m}^{-2} \text{ s}^{-1}$. In general, the magnitude of the fluxes on strings were higher than those representing the micrometeorological tower footprint. For example, on August 4 (DOY 216) the footprint flux was $-0.09 \text{ mg CO}_2 \text{ m}^{-2} \text{ s}^{-1}$ whereas the string flux was $-0.23 \text{ mg CO}_2 \text{ m}^{-2} \text{ s}^{-1}$. Such differences have been reported previously for northern peatlands and are usually attributed to the greater distance to the water table and, hence, a larger zone of aerobic respiration, in the string areas.

An exponential relationship was found between the mid-season surface CO_2 fluxes and the 0.1 m peat temperatures in 1994. The relationship yielded an apparent Q_{10} close to two. There appeared to be higher CO_2 fluxes from all areas immediately following precipitation events. Our 1994 measurements agreed well with the results from August and September, 1993. The 1994 values are also comparable to those we obtained in 1994 in a mid-latitude prairie marsh in western Nebraska (open water fluxes of -0.03 to $-0.13 \text{ mg CO}_2 \text{ m}^{-2} \text{ s}^{-1}$ in *Phragmites*-dominated communities and -0.03 to $-0.09 \text{ mg CO}_2 \text{ m}^{-2} \text{ s}^{-1}$ in *Scirpus*-dominated communities).

Surface fluxes were determined from mid-May through early October, 1995 at the twelve 1993 platform locations. Again, six of the twelve platforms were in vegetation communities representative of the micrometeorological footprint of the eddy correlation flux sensors and six were located in strings which, in general, were areas with a greater distance to the water table. While the

strings comprise a very small proportion of the tower footprint, they are quite common in the northern half of the fen and are the reason this fen is classified as a patterned peatland.

The surface CO₂ flux was consistently greater in *Larix*-dominated (large) strings than in the lower lying *Betula*- or *Carex*-dominated areas (Fig. 12). Individual early season (DOY 152-189) values ranged from 0 to -0.44 mg CO₂ m⁻² s⁻¹ for strings and from 0 to -0.26 mg CO₂ m⁻² s⁻¹ for the lower-lying areas. The fluxes were positively correlated with peat temperatures at 0.1 m below the surface in both strings and lower areas. On strings, the flux at 25°C (peat temperature) increased from -0.08 to -0.23 mg CO₂ m⁻² s⁻¹ as the depth to the water table increased from 0 to >0.2 m. A similar, though less pronounced, trend was seen in lower areas where fluxes at 25°C (peat temperature) increased from -0.06 to -0.12 mg CO₂ m⁻² s⁻¹ as the depth to the water table increased from 0 to 0.1 m. The diel pattern of the surface CO₂ flux reflected the diel pattern of the 0.1 m peat temperature.

Seasonal patterns of surface fluxes in 1995 (Fig. 12A) indicated that fluxes were relatively small early in the season (*e.g.*, -0.04 and -0.06 mg CO₂ m⁻² s⁻¹ on DOY 133 [May 13] for footprint and string areas, respectively). Mean midseason values were near -0.12 and -0.22 mg CO₂ m⁻² s⁻¹ for footprint and string areas, respectively. Mean surface fluxes declined late in the season and were -0.05 and -0.08 mg CO₂ m⁻² s⁻¹ on DOY 276 (October 3). The 0.1 m peat temperatures were also low early and late in the season (*ca.* 6-9°C, see Fig. 12B) while midseason values were generally higher (*ca.* 14 -18°C). The magnitudes of the fluxes from the strings were, in general, greater than those from the footprint areas. These differences are due, in part, to the greater distance to the water table in the string areas (Fig. 12C). We obtained similar results from the 1994 growing season.

We segregated the surface fluxes according to distance to the water table and plotted them as a function of the 0.1 m peat temperature (Fig. 13). Exponential equations fit to the data had Q_{10} factors ranging from 1.9 to 2.7. As in 1994, the relationships with peat temperature depended not only on the distance to the water table, but also on whether the flux was from a string or a footprint area. Again, the strings exhibited greater surface fluxes, possibly due to the greater leaf area indices in these areas.

The 1995 data agreed well with results from previous years. Over all three years, string fluxes were typically between -0.05 and $-0.40 \text{ mg CO}_2 \text{ m}^{-2} \text{ s}^{-1}$ and footprint fluxes ranged from -0.04 to $-0.20 \text{ mg CO}_2 \text{ m}^{-2} \text{ s}^{-1}$.

3.3 CHAMBER MEASUREMENTS OF INDIVIDUAL LEAF GAS EXCHANGE

Leaf photosynthesis, stomatal conductance and respiration measurements were made using a portable gas exchange system (LI-6200, Li-Cor, Inc., Lincoln, Nebraska). A 0.25 liter measurement chamber was used. Gas exchange measurements were focused on *Betula pumila* and *Menyanthes trifoliata* based on the relative abundance of these species in the fen and their relatively large leaves. A limited set of measurements was made on leaves of *Carex* species. Leaf areas were determined with a small ruler in the field. The *Betula* leaves were assumed to be circular. Boundary layer conductances were determined by using moistened filter paper leaf replicas enclosed in the measurement chamber.

Leaf optical properties were determined during the 1993 pilot study in collaboration with Dr. E. A. Walter-Shea. Leaves were placed in an integrating sphere and optical properties were determined with an SE-590 spectroradiometer. Absorptances for both species were high. The mean absorptance of the adaxial surface of *Betula pumila* leaves was 0.85 while that of *Menyanthes*

trifoliata was 0.84 (Table 2). These values were used to convert incident PAR to absorbed PAR for the various response curves.

Responses of CO₂ assimilation rates to absorbed light intensity were determined in 1993 by making measurements on selected leaves in the canopy which had a wide range of incident light intensities. In subsequent years, an external light source was used so that a light response curve could be obtained from a single leaf. Leaf gas exchange measurements were made in August, 1993, early June through late August, 1994 and early June through late September, 1995.

The light response curves for net CO₂ assimilation and stomatal conductance for each species were similar for all three years. A typical set of measurements is shown in Figure 14. Peak mid-season assimilation rates for both *Betula pumila* and *Menyanthes trifoliata* were near 20 $\mu\text{mol CO}_2 \text{ m}^{-2} \text{ s}^{-1}$ while *Carex* exhibited smaller peak rates closer to 11 $\mu\text{mol CO}_2 \text{ m}^{-2} \text{ s}^{-1}$. [Note: 1 $\mu\text{mol CO}_2 \text{ m}^{-2} \text{ s}^{-1} = 0.044 \text{ mg CO}_2 \text{ m}^{-2} \text{ s}^{-1}$.] Full sunlight rates obtained earlier and later in the season tended to be smaller (e.g., 9-11 $\mu\text{mol CO}_2 \text{ m}^{-2} \text{ s}^{-1}$ for *Betula* in early June and late August). The light curves appeared to saturate at light intensities above 1000 $\mu\text{mol quanta m}^{-2} \text{ s}^{-1}$ in all three species with *Betula* typically exhibiting somewhat less pronounced saturation than the other two species (see Fig. 14). Light compensation points occurred near 50 $\mu\text{mol quanta m}^{-2} \text{ s}^{-1}$ in all three species. Stomatal conductances corresponding to the peak mid-season full sunlight assimilation rates were 0.6 $\text{mol H}_2\text{O m}^{-2} \text{ s}^{-1}$ for *Menyanthes*, 0.4 $\text{mol H}_2\text{O m}^{-2} \text{ s}^{-1}$ for *Betula* and 0.25 $\text{mol H}_2\text{O m}^{-2} \text{ s}^{-1}$ for *Carex*. In parallel with the CO₂ assimilation rates, maximum stomatal conductances were smaller earlier and later in the growing season (e.g., 0.2 $\text{mol H}_2\text{O m}^{-2} \text{ s}^{-1}$ for *Betula* in early June and late August).

Responses of net CO₂ assimilation rates to internal CO₂ concentration (A-C_i curves) in *Betula* and *Menyanthes* were typical of other C₃ plant species. Initial slopes (carboxylation

efficiencies) and C_i at ambient CO_2 concentrations were dependent upon incident light intensity. Under full sunlight, at ambient CO_2 concentrations (ca. 350 ppm) the C_i values for both *Betula* and *Menyanthes* ranged from 200 to 250 ppm.

Single leaf respiration rates were determined during the day by enclosing the leaves in opaque bags and allowing the CO_2 exchange rates to stabilize (usually 5-15 min). We determined most of our respiration measurements during the 1994 season with limited measurements during 1993 and 1995. For most of our investigations there were no significant differences in single leaf respiration rates expressed on a leaf area basis for the three dominant species (Fig. 15). However, in 1993 we found slightly higher (more negative) respiration rates in *Menyanthes* than in *Betula*. For example, at 25°C, the respiration rate in *Menyanthes* was $-2.2 \mu\text{mol CO}_2 \text{ m}^{-2} \text{ s}^{-1}$ while in *Betula* it was $-2.0 \mu\text{mol CO}_2 \text{ m}^{-2} \text{ s}^{-1}$. In all cases, the respiration rates increased exponentially with leaf temperature. The apparent Q_{10} s for these relationships were near two. For the fitted curve shown in Fig. 15 the equation was: respiration rate ($\text{mg CO}_2 \text{ m}^{-2} \text{ s}^{-1}$) = $-0.0921 \exp [44934 (T_{\text{leaf}} - 25) / ((298) (8.314) (T_{\text{leaf}} + 273))]$.

The single leaf gas exchange properties, particularly stomatal conductance values, exhibited a fair amount of variability over the course of the growing season, and, at times, over the course of a day. We investigated this further in 1995. Diurnal patterns of individual leaf gas exchange properties for *Betula* and *Menyanthes* were determined on several selected days during the 1995 season (see, e.g., Fig. 16). We often observed the largest stomatal conductances and net CO_2 assimilation rates very early in the morning with declining (later steady) values later in the day. In Fig. 16, the maximum stomatal conductance was recorded at about 0830 CST when the air relative humidity (RH) was high (60%) and the leaf-to-air vapor pressure deficit (VPD) was low (1.5 kPa). Although the incident light intensity was relatively constant during the measurement period, both

stomatal conductance and net CO₂ assimilation rate declined throughout the morning hours. A slight increase in stomatal conductance was noted on this day (August 5, 1995, DOY 217); however, this recovery did not appear consistently in all data sets. In other species, these strong diurnal patterns have been correlated with diurnal changes in VPD. We determined the responses of gas exchange properties to VPD for *Menyanthes* and *Betula* using a steady-state gas exchange system (LI-6400, Li-Cor, Inc., Lincoln NE). The leaf stomatal conductance for both species appeared to be strongly influenced by VPD (Fig. 17) with values decreasing by roughly 50% as the VPD increased from 1.0 to 3.5 kPa. Increasing VPD caused somewhat smaller decreases in net CO₂ assimilation rates due to concomitant changes in leaf internal CO₂ concentration.

Over all three years, we obtained fairly consistent results for the leaf gas exchange parameters we measured. Both the net CO₂ assimilation rates and the stomatal conductances for *Betula*, *Menyanthes* and *Carex* were of the same order of magnitude that we have measured in other native C₃ plants growing in relatively undisturbed locations. For example, the gas exchange properties discussed above are similar to values obtained from *Phragmites australis* and *Scirpus acutus* in a western Nebraska marsh and *Scheuchzeria palustris* in a northern Minnesota peatland. The diurnal dependence on VPD also seems typical for native species; our results from *Phragmites* also exhibited this behavior. However, by way of comparison, for cultivated C₄ species (*e.g.*, maize, sorghum), we typically observe much higher net CO₂ assimilation rates (60 μmol CO₂ m⁻² s⁻¹) and stomatal conductances (0.8 mol H₂O m⁻² s⁻¹). The cultivated species also appear to be less sensitive to diurnal changes in VPD.

3.4 CHAMBER METHANE FLUX AND ASSOCIATED MEASUREMENTS

In 1994, we investigated the environmental factors controlling CH_4 emissions from wetlands. This effort had two main components: (a) an analysis of temporal and spatial relationships between CH_4 emissions and controlling variables such as water table and temperature; and (b) experimental analysis of the impact of manipulated peat chemistry on rates of CH_4 emissions. This section summarizes these analyses, first focusing on the temporal and spatial patterns, and then on the experimental responses.

Spatial and Temporal Dynamics

All static chamber measurements were performed near four platforms (along the two transects discussed earlier), at which water table relative to average peat surface was also measured. Each of the four platforms is identified by a two letter code indicating the transect (north or south) and the location (A or B) along the transect. The water table levels were referenced to the average peat surface obtained by mapping the elevation of the peat surface at each plot. As each platform was visited once per week on average, and never on the same day as another platform, we constructed a synthetic hydrograph for the season at each platform by assuming that the water table was level and fluctuated uniformly (*i.e.*, moved up and down as a plane) across the site. The resulting hydrographs (Fig. 18) were highly correlated ($r = 0.96$) with the pattern generated by a continuously recording "bog shoe" operated near the eddy correlation tower, supporting the assumption of uniformly fluctuating water table and use of the synthetic, platform-specific hydrographs. During the course of the season, CH_4 emissions at one of the platforms ("NA") were consistently much smaller than at the other three (Fig 19). Comparison of the water table measurements (Fig 18.) indicated that the peat surface at the NA platform was nearly 5 cm higher

than at the other platforms, which confirmed our impression that the surface peat there was somewhat drier than elsewhere. It is tempting to speculate that an extra 5 cm of aerobic peat oxidized much of the CH_4 passing through it and therefore accounted for the observed differences, but the picture is somewhat more complicated. Temporal water table fluctuations were much higher (~23 cm, max to min) than any differences among locations, and the average peat surface at NA was below the water table for about 50 days (compared to the entire growing season at the other platforms). Thus, the temporal effects of water table dynamics on CH_4 were strongly mitigated by their long-term averages, perhaps through effects on the near-surface redox and peat chemistry.

We do not know why the peat surface was higher at the NA platform than at other platforms. Above-ground biomass at the end of the growing season was about average (Table 3), and estimated net primary productivity (based on estimate of current season biomass) was lower than at the other platforms. Two remaining possibilities — from which we have no basis to choose — are that 1) low organic matter quality at NA slowed decomposition, or 2) the peat surface has undergone uplift due to hydrologic flow (similar to string formation). Because the NA platform emissions pattern was so strikingly different from those at the other three platforms (which showed very good consistency), data from this platform were excluded from statistical analyses and much of the following discussion (although they are included in the figures for completeness).

Figure 19 shows the CH_4 fluxes measured by the static chambers and the eddy correlation technique. August 11 and 22 (DOY 223 and 234, indicated by circled triangles) had light rainfall in the morning and following the rain, the flux was by about 50% larger than the previous day. The eddy correlation measurements declined less rapidly than their static chamber counterparts following peak emission rates. Nonetheless, the overall correspondence in magnitudes and the temporal patterns of CH_4 fluxes measured by the static chambers and the eddy correlation technique

was good ($r = 0.83$). Also, methane fluxes paralleled changes in both peat temperature and water table (Fig. 19B).

Experimental Manipulation Results

Our 1994 field efforts concentrated on modifying key characteristics of the peat chemistry underneath the chamber measurement sites using a factorial combination of low quality carbon (C, as wheat straw) and nitrogen (N, as urea) amendments in order to identify and quantify driving variables governing CH_4 effluxes in the SSA fen. We have analyzed these data using two statistical approaches. Based on an ANOVA of all the weekly flux data for the growing season, we found that the sites receiving the nitrogen additions, both with and without C, emitted slightly but significantly more CH_4 ($p < .05$) than did other sites C (Fig. 20). Two mechanisms may account for this difference: a) added N enhanced the rate of CH_4 production by enhancing fermentability of organic matter, or b) added N reduced the rate of CH_4 oxidation in the aerobic peat overlying the water table. Our index of litter decomposition indicated that N additions increased rates of mass loss and N accumulation ($p < .05$) of wheat straw residues, potentially accelerating the rate at which C substrates became available to methanogenic population and supporting hypothesis (a).

The second approach involved an analysis of the integral seasonal CH_4 emission total by replicate, as opposed to the individual weekly fluxes. With only three resulting replicates (four if the NA replicate is included), the differences between the “no N” and “added N” treatments were no longer significant at $p < 0.05$.

Acceleration of CH_4 emissions by added N would have important implications for likely responses of wetland CH_4 emissions to changes in N availability resulting from changes in climate or nitrogen deposition rates. Our results suggest that increasing N availability may accelerate the

rate of peat decomposition, which under anaerobic conditions also promotes greater CH₄ production rates. Our modeling effort incorporates peat decomposability (as C quality) as well as temperature and water table dynamics in determining CH₄ fluxes. Because of its consistent importance in modeling (Valentine *et al.*, 1994a,b), we believe that the consideration of peat chemistry will be essential to understanding and predicting variability in CH₄ emissions in both time and space, both now and in response to future environmental change.

At the Trace Gas Network workshop (Santa Barbara, CA) in December, 1997, we began work with Ms. Bernadette Walter, a Ph.D. candidate at the Max Plank Institute, on testing her global methane emissions model using our results. Using relatively simple parameters, her model has already demonstrated outstanding fit to existing wetland CH₄ emission data. Because her model's data requirements are better matched by our data than data previously available, this will offer an excellent opportunity to examine how well this model will work at a global level.

4. SCIENTIFIC PUBLICATIONS STEMMING FROM THIS PROJECT

4.1 JOURNAL ARTICLES

Arkebauer, T. J. and E. C. Jolitz. 1998. Soil surface carbon dioxide exchange in a boreal fen (in preparation).

Arkebauer, T. J. 1998. Gas exchange properties of *Betula pumila* and *Menyanthes trifoliata* in a boreal fen (in preparation).

Frolking, S., J. Bubier, T. Moore, L. Bellisario, P. Carroll, P. Crill, P. Lafleur, H. McGaughey, N. Roulet, S. B. Verma, A. E. Suyker, M. Waddington, G. Whiting, T. Ball, A. Bhardwaj. 1998. The relationship between photosynthetically active radiation and ecosystem productivity for seven northern peatlands. *Global Biogeochem. Cycles* (in press).

- Suyker, A. E., S. B. Verma, R. J. Clement and D. P. Billesbach. 1996. Methane flux in a boreal fen: season-long measurement by eddy correlation. *J. Geophys. Res.* 101(22):28,637-28,647.
- Suyker, A. E., S. B. Verma and T. J. Arkebauer. 1997. Season-long measurement of carbon dioxide exchange in a boreal fen. *J. Geophys. Res.* 102(D24):29,021-29,028.
- Suyker, A. E., S. B. Verma, D. B. Billesbach and R. J. Clement. 1998. Methane flux in a boreal fen: an analysis of measurements during two consecutive growing seasons (in preparation).
- Suyker, A. E. and S. B. Verma. 1998. Two growing seasons of CO₂ exchange in a boreal wetland (in preparation).
- Suyker, A. E. and S. B. Verma. 1998. Energy exchange in a boreal wetland (in preparation).
- Valentine, D. W. and W. M. Pulliam. 1998. Influence of substrate characteristics and other environmental factors on methane emissions from the BOREAS Southern Study Area fen site (in preparation).

4.2 PAPERS PRESENTED

- Suyker, A. E., S. B. Verma, R. J. Clement and D. P. Billesbach. 1995. Methane flux by eddy correlation from a boreal fen. American Geophysical Union Spring Meeting, May 30-31, 1995, Baltimore, MD.
- Suyker, A. E., S. B. Verma and T. J. Arkebauer. 1996. Carbon dioxide exchange in a boreal fen. Presented at the 22nd Conference for Agricultural & Forest Meteorology of the American Meteorological Society, January 28-February 2, 1996, Atlanta, GA.

Arkebauer, T. J., E. C. Jolitz and S. B. Verma. 1996. Soil surface CO₂ flux in a boreal fen.

Presented at the 22nd Conference for Agricultural & Forest Meteorology of the American Meteorological Society, January 28-February 2, 1996, Atlanta, GA.

Valentine, D. W. 1996. Ecosystem controls on CH₄ production and emission in northern wetlands: insights to be gained from use of stable isotopes in passed gas. Invited seminar to the UAF's Institute of Arctic Biology science seminar series.

Valentine, D. W., W. M. Pulliam, E. A. Holland and D. S. Schimel. 1997. Biogeochemical constraints on CH₄ emissions from northern fens. Oral presentation, International Symposium on Seasonally Frozen Soils, June 10-12, 1997.

Valentine, D. W. 1997. Ecosystem controls over methane emissions in the BOREAS Southern Study Area fen. Oral presentation, Ecological Society of America annual meeting.

5. REFERENCES

- Alm, J., A. Talanov, S. Saarnio, J. Silvola, E. Ikkonen, H. Aaltonen, H. Nykanen, and P. J. Martikainen, Reconstruction of the carbon balance for microsites in a boreal oligotrophic pine fen, Finland, *Oecologia*, 110, 423-431, 1997.
- Baldocchi, D. D., C. A. Vogel, and B. Hall, Seasonal variation of carbon dioxide exchange rates above and below a boreal jackpine forest, *Agric. For. Meteorol.*, 83, 147-170, 1997.
- Billings, W. D., J. O. Luken, D. A. Mortenson, and K. M. Peterson, Arctic tundra: A source or sink for atmospheric carbon dioxide in a changing environment, *Oecologia*, 53, 7-11, 1982.
- Billings, W. D., J. O. Luken, D. A. Mortenson, and K. M. Peterson, Increasing atmospheric carbon dioxide: Possible effects on Arctic tundra, *Oecologia*, 58, 286-289, 1983.
- Bubier, J. L., T. R. Moore, L. Bellisario, N. T. Comer, and P. M. Crill, Ecological controls on methane emissions from a northern peatland complex in the zone of discontinuous permafrost, Manitoba, Canada, *Global Biogeochem. Cycles*, 9 (4), 455-470, 1995.
- Bubier, J. L., T. R. Moore, and N. T. Roulet, Methane emissions from wetlands in the mid boreal region in northern Ontario, *Ecology*, (74), 2240-2254, 1993.
- Crill, P. M., K. B. Bartlett, and N. Roulet, Methane flux from boreal peatlands, *Soil Sci. Soc. Am. J.*, 43, 173-182, 1988.
- Dise, N. B., E. Gorham, and E. Verry, Environmental factors controlling methane emissions from peatlands in northern Minnesota, *J. Geophys. Res.* 98, 10,583-10,594, 1993.
- Fan, S.-M., M. L. Goulden, J. W. Munger, B. C. Daube, P. S. Bakwin, S. C. Wofsy, J. S. Amthor, D. R. Fitzjarrald, K. E. Moore, and T. R. Moore, Environmental controls on the photosynthesis and respiration of a boreal lichen woodland: A growing season of whole ecosystem exchange measurements by eddy correlation, *Oecologia*, 102(4), 443-452, 1995.
- Freeman, C., M. A. Lock, and B. Reynolds, Fluxes of CO₂, CH₄, and N₂O from a Welsh peatland following simulation of water table draw-down: potential feedback to climatic change, *Biogeochem.*, 19, 51-60, 1993.
- Frolking, S., and P. Crill, Climate controls on temporal variability of methane flux from a poor fen in southeastern New Hampshire: Measurement and modeling, *Global Biogeochem. Cycles*, 8, 385-397, 1994.
- Frolking, S., J. Bubier, T. Moore, L. Bellisario, P. Carroll, P. Crill, P. Lafleur, H. McCaughey, N. Roulet, S. B. Verma, A. E. Suyker, M. Waddington, G. Whiting, T. Ball, and A. Bhardwaj, The relationship between photosynthetically active radiation and ecosystem productivity for seven northern peatlands, *Global Biogeochem. Cycles* 1998 (in press).

- Funk, D. W., E. R. Pullman, K. M. Peterson, P. M. Crill, and W. D. Billings, Influence of water table on carbon dioxide, carbon monoxide, and methane fluxes from taiga bog microcosms, *Global Biogeochem. Cycles*, 8(3), 271-278, 1994.
- Jarvis, P. G., J. B. Moncrieff, J. M. Massheder, M. B. Rayment, S. E. Hale, and S. L. Scott, Carbon dioxide exchange of boreal forest in BOREAS, final report, *TIGER Spec. Proj. GST/02/619* and *SGT/02/984*, Univ. of Edinburgh, 1995.
- Moore, T. R., and M. Dalva, The influence of temperature and water table position on carbon dioxide and methane emissions from laboratory columns of peatland soils, *J. Soil Science*, 44, 651-664, 1993.
- Mosier, A. R., L. K. Klemetsson, R. A. Sommerfeld, and R. C. Musselman, Methane and nitrous oxide flux in a Wyoming subalpine meadow. *Global Biogeochemical Cycles* 7 (4), 771-784, 1993.
- Nykanen, H., J. Alm, J. Silvola, and P. J. Martikainen, Fluxes of methane in boreal mires with different hydrology and fertility in Finland, in *Northern Peatlands in Global Climatic Change*, Proceedings of the International Workshop held in Hyytiala, Finland, 8-12 October, 1995, edited by R. Laiho *et al.*, pp 127-135, Publications of the Academy of Finland 1/96, Edita, Helsinki, Finland, 1996.
- Roulet, N. T., A. Jano, C. A. Kelly, L. F. Klinger, T. R. Moore, R. Protz, J. A. Ritter, and W. R. Rouse, The role of Hudson Bay lowland as a source of atmospheric methane, *J. Geophys. Res.*, 99, 1439-1454, 1994.
- Oechel, W. C., and W. D. Billings, Effects of global change on the carbon balance of Arctic plants and ecosystems, in *Arctic Ecosystems in a Changing Climate*, edited by F. S. Chapin III *et al.*, pp 139-168, Academic, San Diego, Calif., 1992.
- Saarnio, S., J. Alm, J. Silvola, A-L. Lohila, H. Nykanen, and P. J. Martikainen, Seasonal variation in methane emissions and production and oxidation potentials at microsites on an oligotrophic pine fen, *Oecologia*, 110, 414-422, 1997.
- Sellers, P., F. Hall, H. Margolis, B. Kelly, D. Baldocchi, G. Den Hartog, J. Cihlar, M. G. Ryan, B. Goodison, P. Crill, K. J. Ranson, D. Lettenmaier, and D. E. Wickland, The Boreal Ecosystem-Atmosphere Study (BOREAS): An overview and early results from the 1994 field year, *Bull. Am. Meteorol. Soc.*, 76, 1549-1577, 1995.
- Shurpali, N. J., S. B. Verma, J. Kim, and T. J. Arkebauer, Carbon dioxide exchange in a peatland ecosystem, *J. Geophys. Res.*, 100(D7), 14,319-14,326, 1995.
- Shurpali, N. J., and S. B. Verma, Micrometeorological measurements of methane flux in a Minnesota peatland during two growing seasons, *Biogeochem.* (submitted).

- Suyker, A. E., and S. B. Verma, Eddy correlation measurements of CO₂ flux using a closed-path sensor: Theory and field tests against an open-path sensor, *Boundary Layer Meteorol.*, 64, 391-407, 1993.
- Suyker, A. E., S. B. Verma, R. J. Clement, and D. B. Billesbach, Methane flux in a boreal fen: Season-long measurement by eddy correlation, *J. Geophys. Res.*, 101(D22), 28,637-28,647, 1996.
- Suyker, A. E., S. B. Verma, and T. J. Arkebauer, Season-long measurement of carbon dioxide exchange in a boreal fen, *J. Geophys. Res.*, 102(D24), 29,021-29,028, 1997.
- Valentine, D. W., E. A. Holland, and D. S. Schimel, Ecosystem and physiological controls over methane production in northern wetlands, *J. Geophys. Res.*, 99D(1), 1563-1571, 1994a.
- Valentine, D. W., L. Klinger, E. A. Holland, and D. S. Schimel, A field experiment of substrate limitation of methane emissions in a northern wetland, *Bull. Ecol. Soc. Am.*, 75(2), 235, 1994b.
- Verma, S. B., Micrometeorological methods for measuring surface fluxes of mass and energy, *Remote Sens. Rev.*, 5(1), 99-115, 1990.
- Whiting, J., CO₂ exchange in the Hudson Bay lowlands: Community characteristics and multi-spectral reflectance properties, *J. Geophys. Res.*, 99, 1519-1529, 1994.

6. TABLES AND FIGURES

Table 1. Model parameters for the CO₂ flux-PAR relationship (Eq. 1) and 95% confidence limits. Here the CO₂ flux is mg m⁻² (leaf area) s⁻¹. Ranges of moderate and high vapor pressure deficit (D) and temperature (T) are defined in the text. During the 1995 season, moderate conditions prevailed most of the time and high D and T were not observed.

Year	Conditions	α mg m ⁻² s ⁻¹ /μmol m ⁻² s ⁻¹	$F_{cL\infty}$ mg m ⁻² s ⁻¹	R_{sL} mg m ⁻² s ⁻¹	r^2
1994	Moderate D&T	0.0009±0.00020	0.68±.05	0.13±0.02	0.74
1995	Moderate D&T	0.0013±0.00022	0.69±.04	0.15±0.02	0.75
1994	High D&T	0.0012±0.0024	0.44±0.19	0.20±0.23	0.38

Table 2. Leaf optical properties for *Betula pumila* and *Menyanthes trifoliata* determined on 19 August, 1993. Numbers are the means (and standard deviations) for the PAR band (400-700 nm).

Species	Surface	n	Reflectance	Transmittance	Absorptance
<i>B. pumila</i>	Adaxial	8	.0878 (.0091)	.0595 (.0127)	.8528 (.0163)
	Abaxial	8	.1665 (.0266)	.0598 (.0126)	.7744 (.0215)
<i>M. trifoliata</i>	Adaxial	8	.1192 (.0484)	.0436 (.0126)	.8373 (.0542)
	Abaxial	8	.1743 (.0387)	.0435 (.0114)	.7822 (.0403)

Table 3. Above-ground standing crop and estimated net primary productivity (ANPP) at the four platforms used for methane efflux controls component. Each datum is an average of 8 0.09 m² quadrats, SE is the standard error of the mean.

Platform	Biomass (mg m ⁻²)	SE	ANPP (mg m ⁻² y ⁻¹)	SE
NA	231	72	110	19
NB	257	87	158	20
SA	229	46	193	33
SB	191	10	189	10

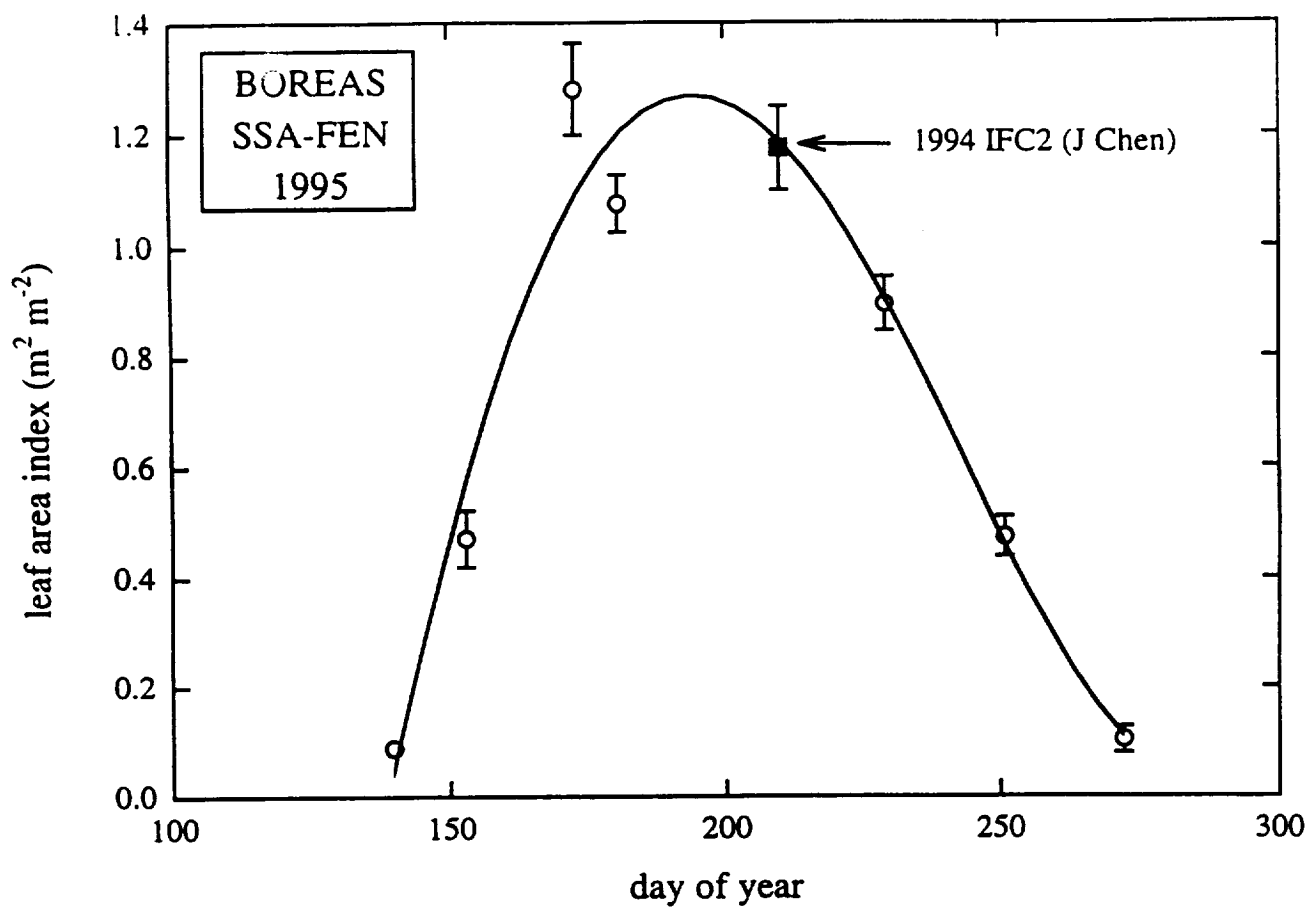


Figure 1. Seasonal course of total green leaf area index (LAI) for the BOREAS SSA-Fen site in 1995. Also shown is the single data point obtained during the 1994 season.

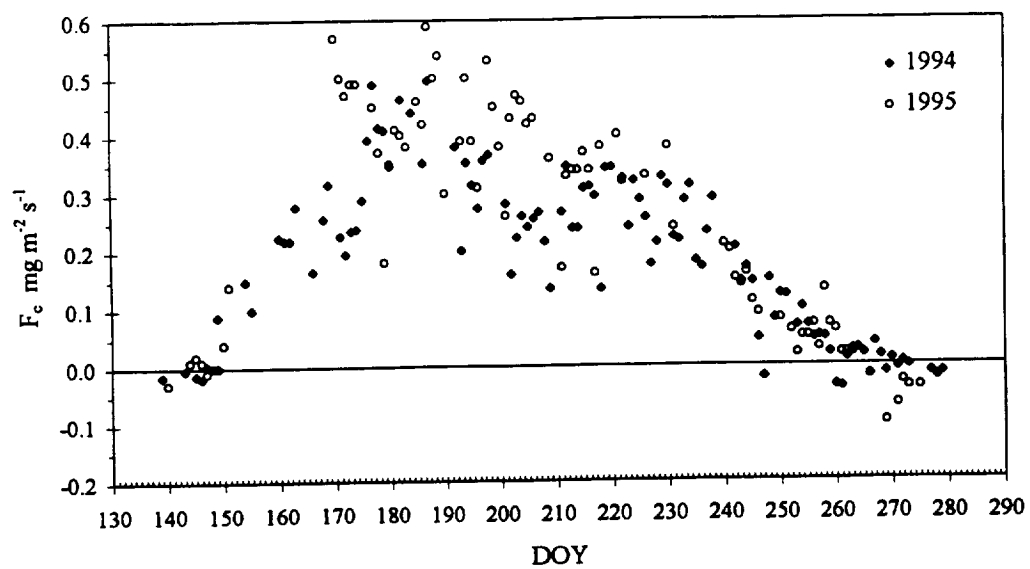


Figure 2. Seasonal patterns of midday (11:30 - 14:30 hr CST) CO₂ flux (F_c) during the 1994 and 1995 growing seasons.

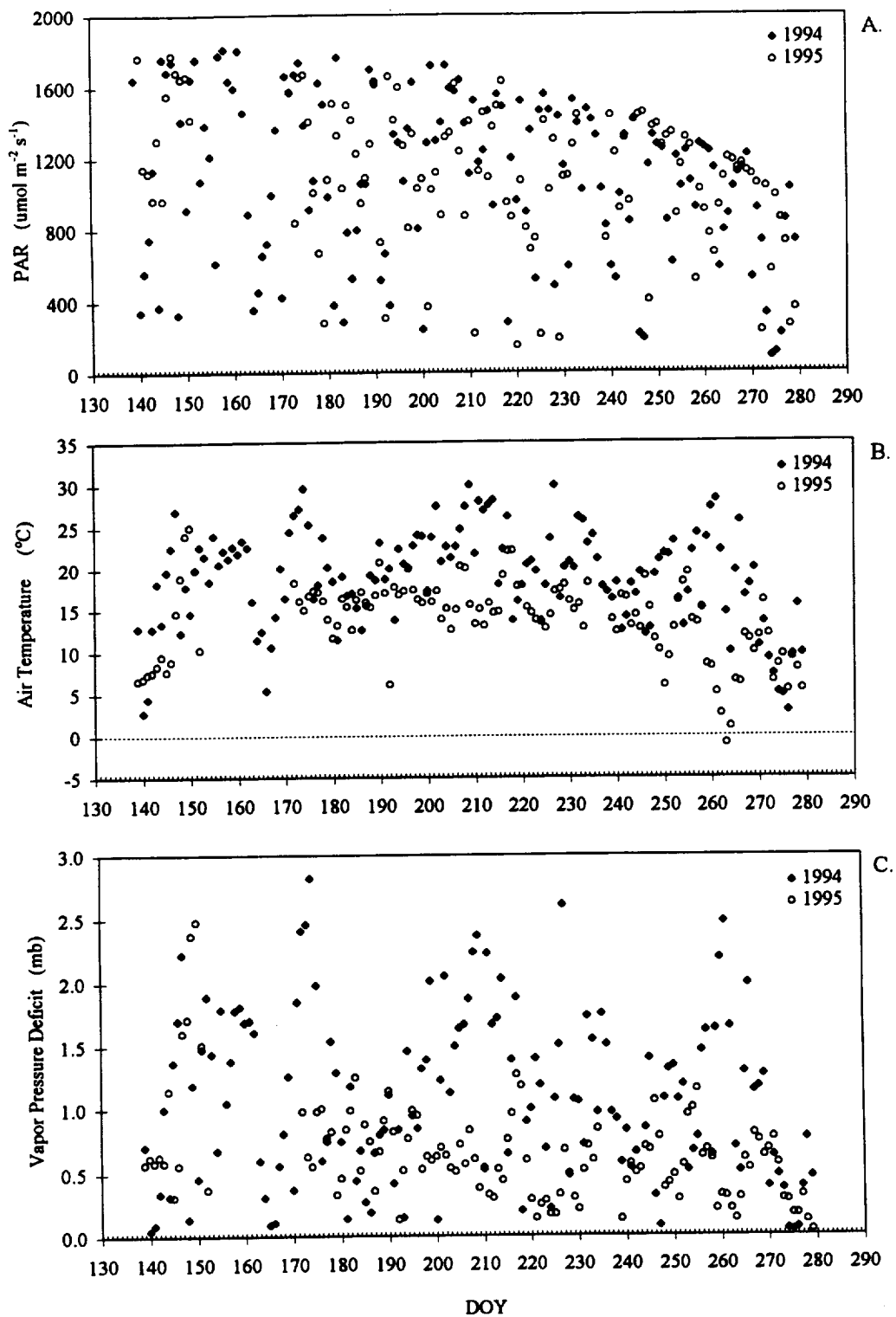


Figure 3. Midday (11:30 - 14:30 hr CST) averages of A) incident photosynthetically active radiation (PAR - $\mu\text{mol m}^{-2} \text{s}^{-1}$), B) air temperature at 4.2m (T - $^{\circ}\text{C}$) and C) vapor pressure deficit at 4.2m (D - mb) during the 1994 and 1995 growing seasons.

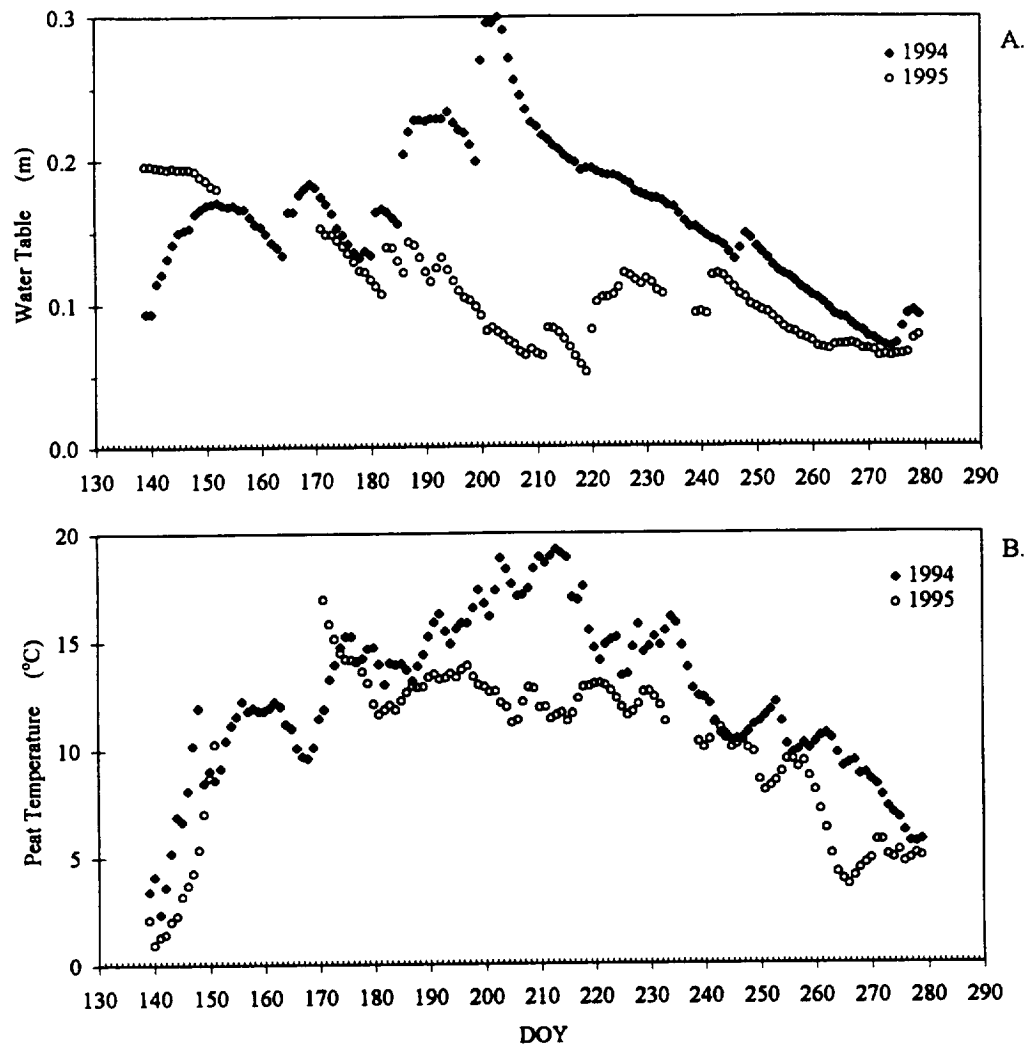


Figure 4. Midday (11:30 - 14:30 hr CST) averages of A) water table above an average hollow surface (W - m), and B) peat temperature 10 cm below an average hollow surface (T_p - °C) during the 1994 and 1995 growing seasons.

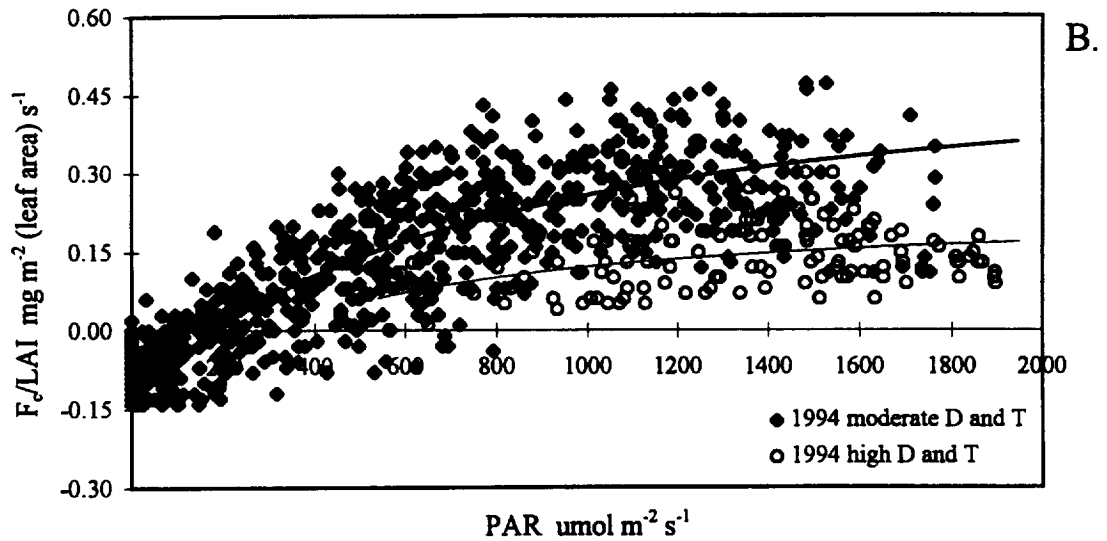
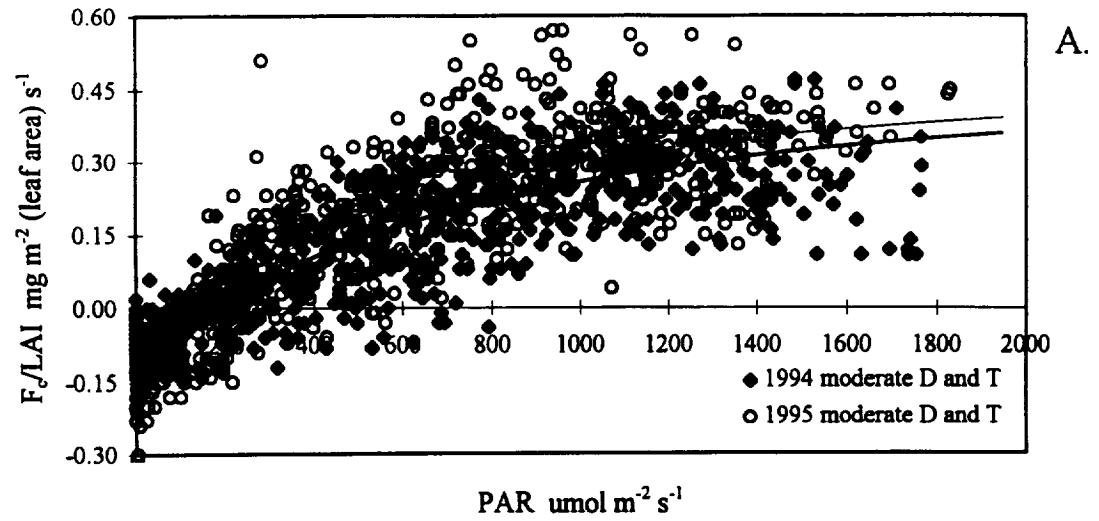


Figure 5. F_c -PAR relationship for A) moderate vapor pressure deficit and temperature in 1994 and 1995 and B) moderate and high vapor pressure deficit and temperature in 1994. A rectangular hyperbola was fit to the data (see text for details). The CO_2 flux is in $\text{mg m}^{-2} (\text{leaf area}) \text{ s}^{-1}$.

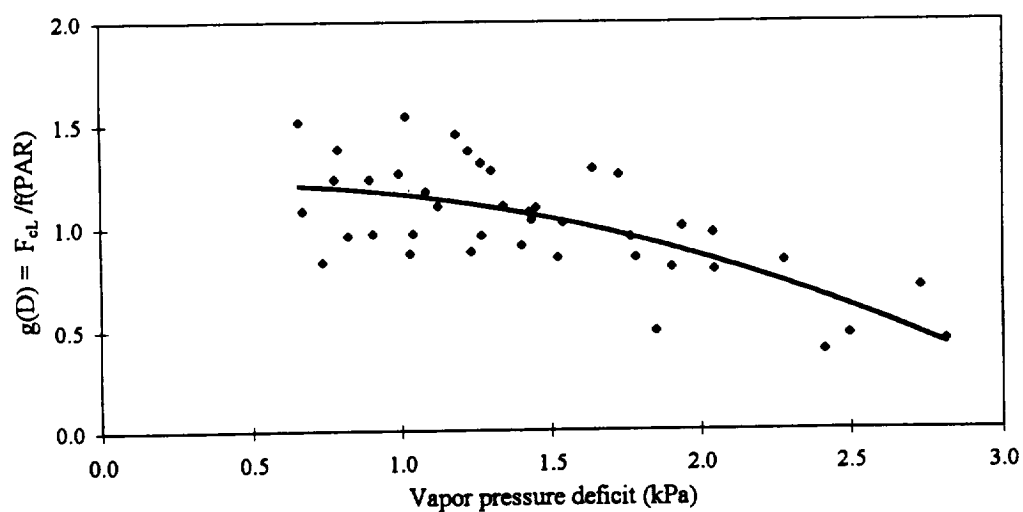


Figure 6. Midday averages (11:30 - 14:30 hr CST) of $g(D)=F_{cl}/f(PAR)$ as a function of the midday average vapor pressure deficit (D) during midseason. The CO_2 flux is in $mg\ m^{-2}\ (leaf\ area)\ s^{-1}$.

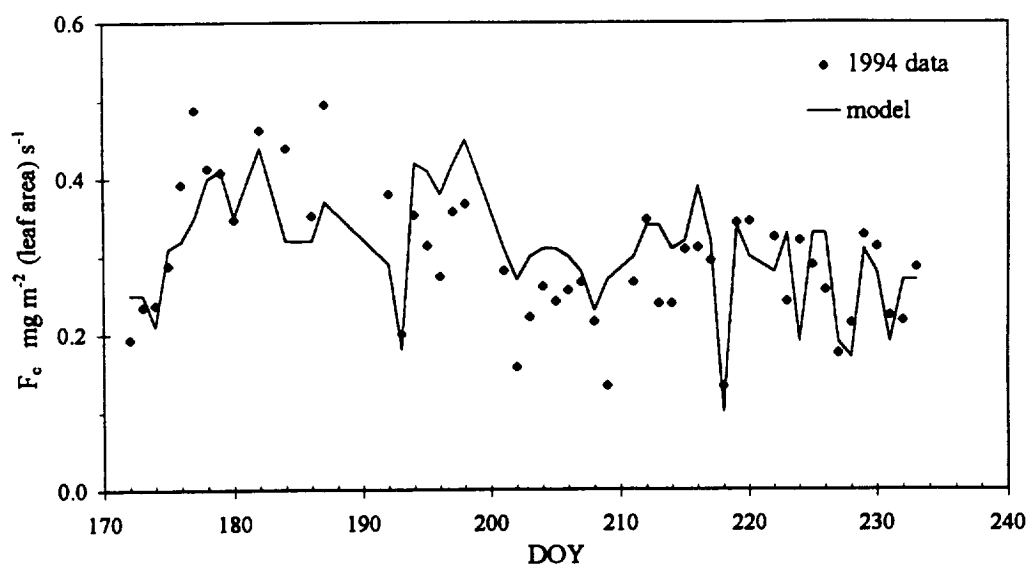


Figure 7. Midday averages (11:30 - 14:30 hr CST) of F_c during June 21-August, 1994 compared to model estimates incorporating high vapor pressure deficit and temperature (see text for details). The CO_2 flux is in mg m^{-2} (leaf area) s^{-1} .

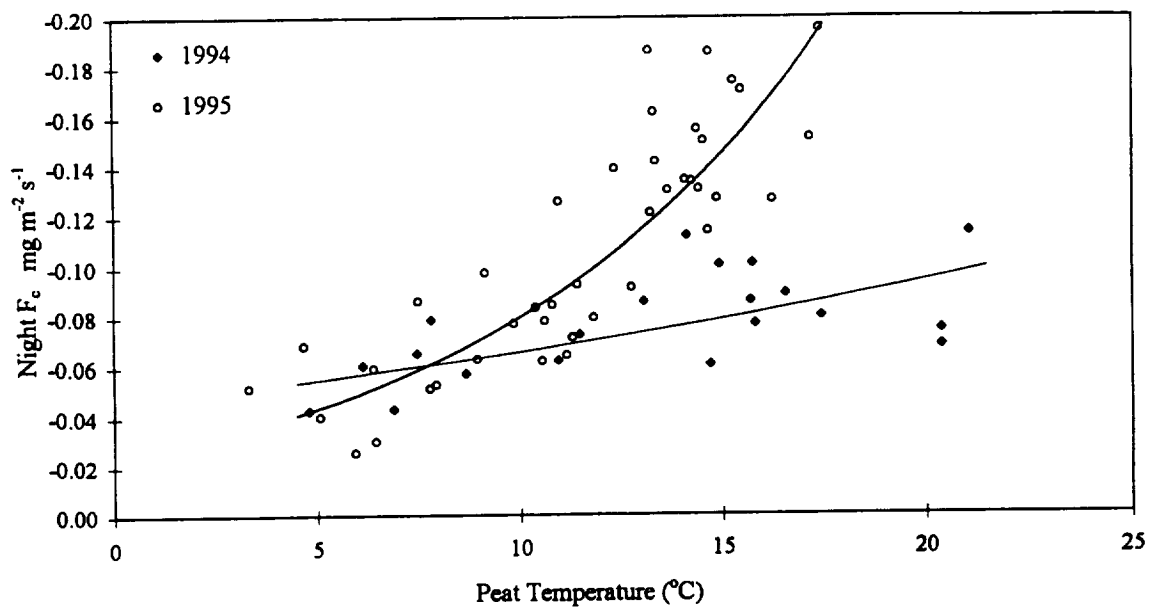


Figure 8. Average nighttime (22:00 - 4:00 hr CST) CO_2 flux (F_c) plotted against peat temperature (T_p) during the 1994 and 1995 growing seasons.

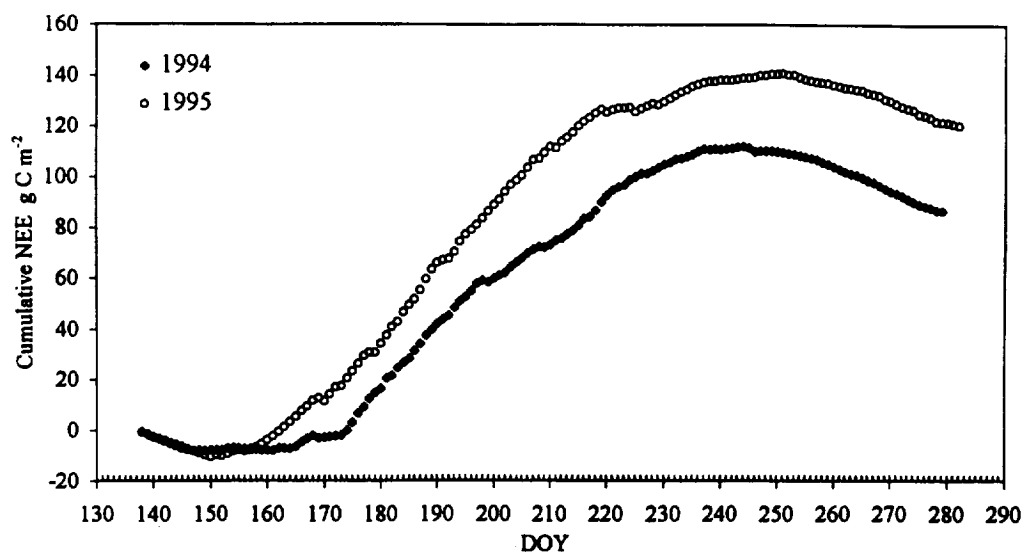


Figure 9. Cumulative net ecosystem CO₂ exchange during the growing seasons of 1994 and 1995.

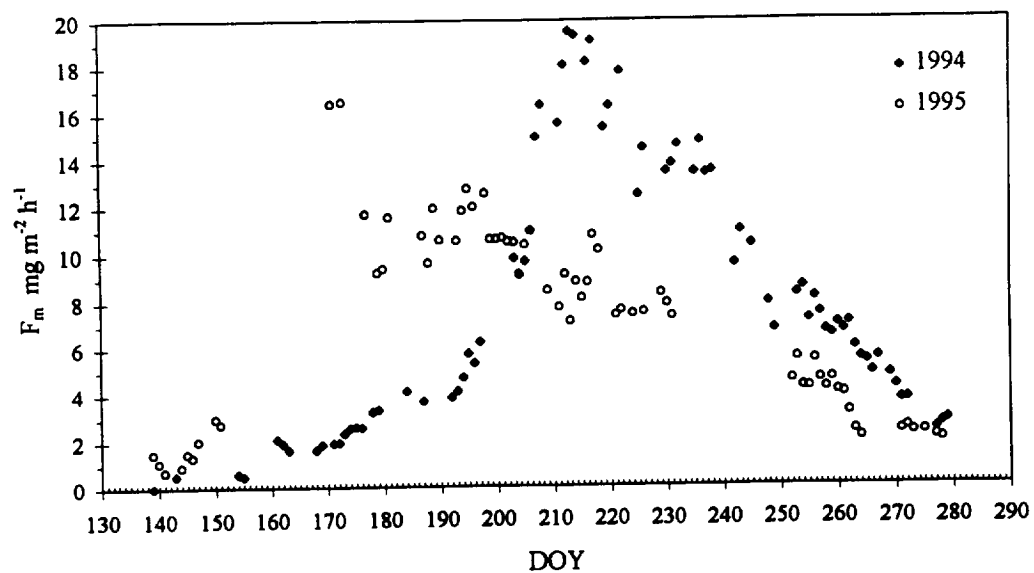


Figure 10. Seasonal patterns of midday (11:30 - 14:30 hr CST) CH₄ flux (F_m) during the growing seasons of 1994 and 1995.

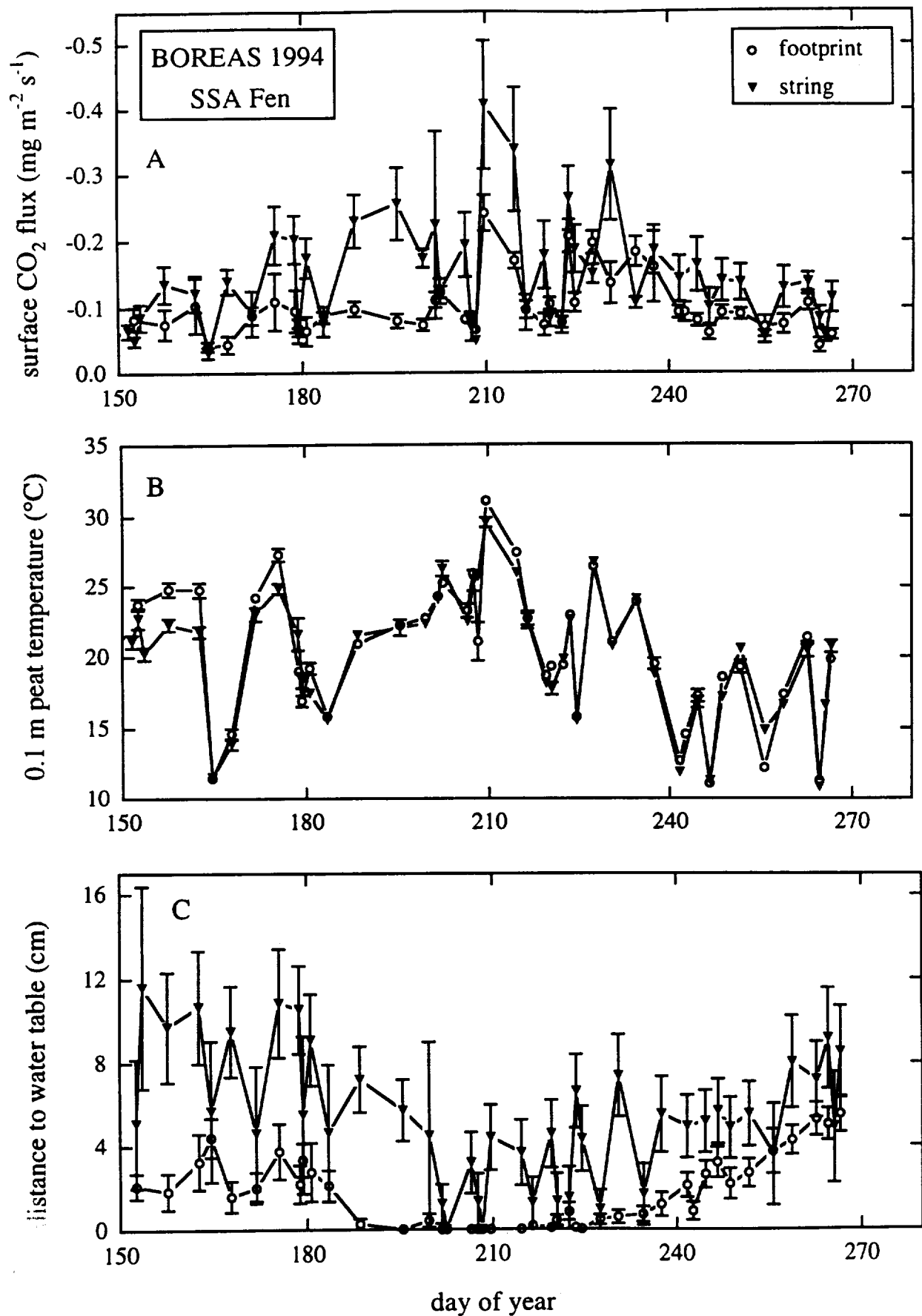


Figure 11. Seasonal course of (A) surface CO₂ flux, (B) 0.1m peat temperature and (C) distance to water table at the BOREAS SSA-Fen site in 1994.

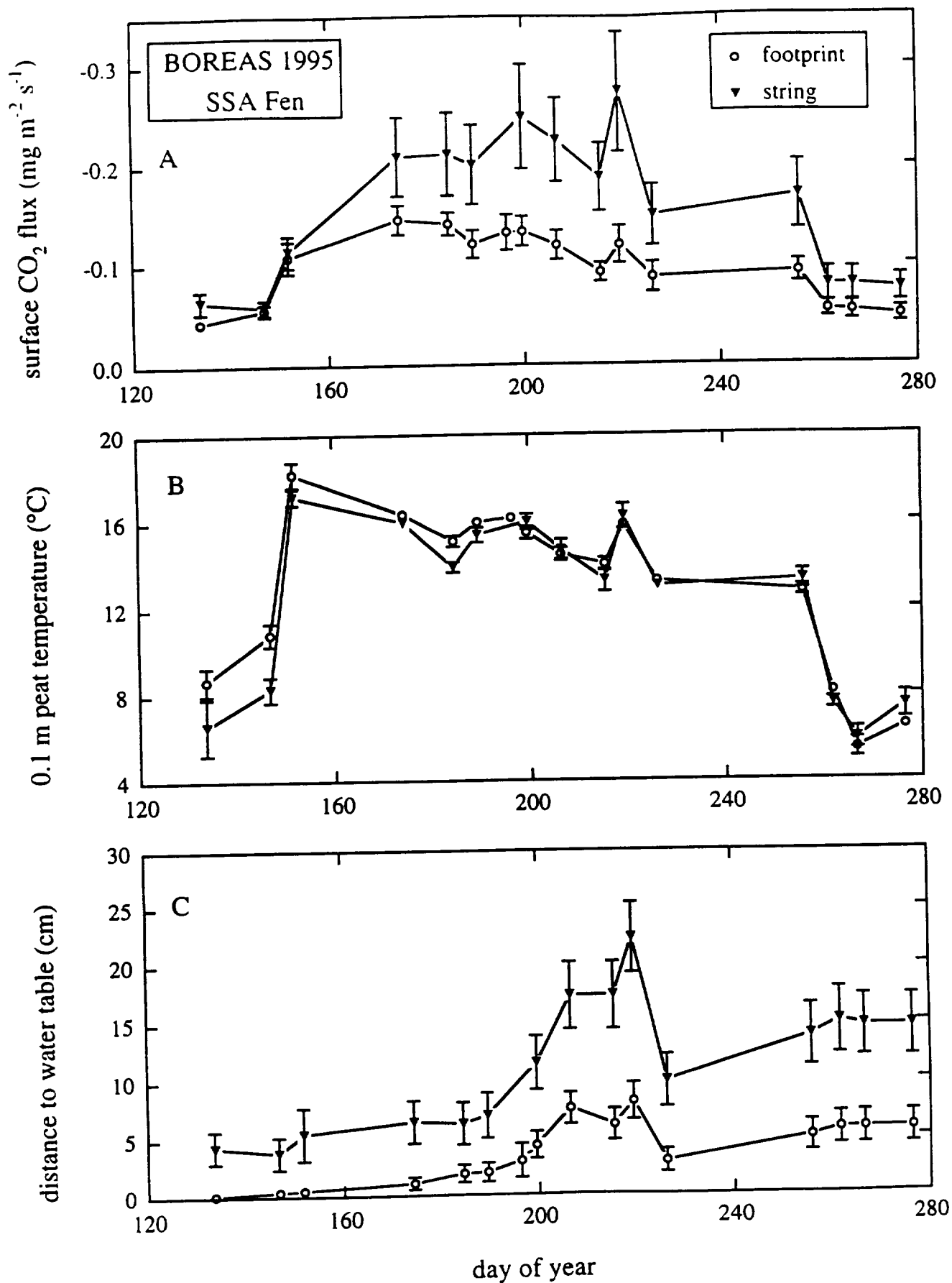


Figure 12. Seasonal course of (A) surface CO₂ flux, (B) 0.1m peat temperature and (C) distance to water table at the BOREAS SSA-Fen site in 1995.

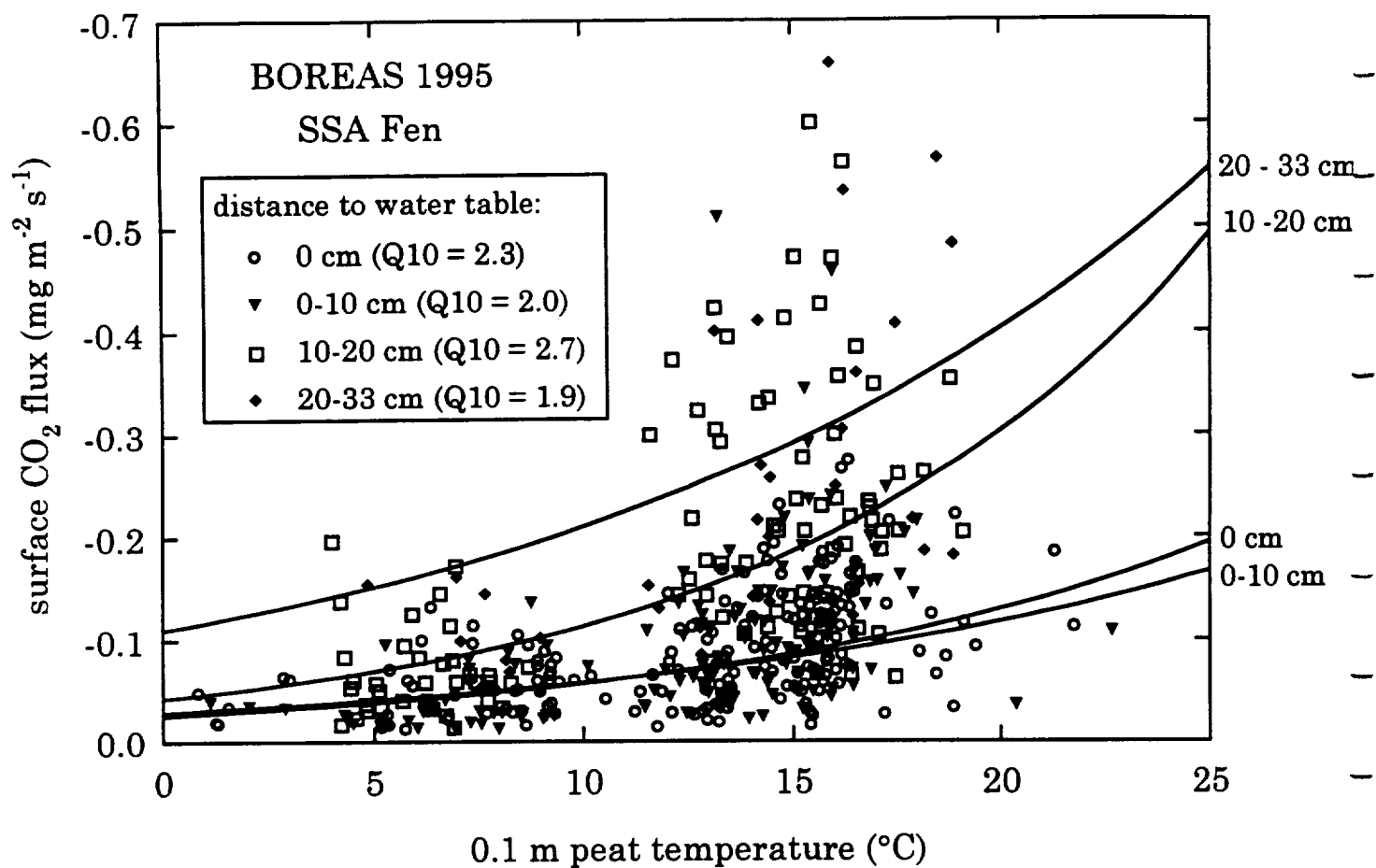


Figure 13. Fitted exponential relationships between individual measurements of surface CO_2 flux and 0.1m peat temperature with data segregated by distance to water table. Data are from the BOREAS SSA-Fen site in 1995.

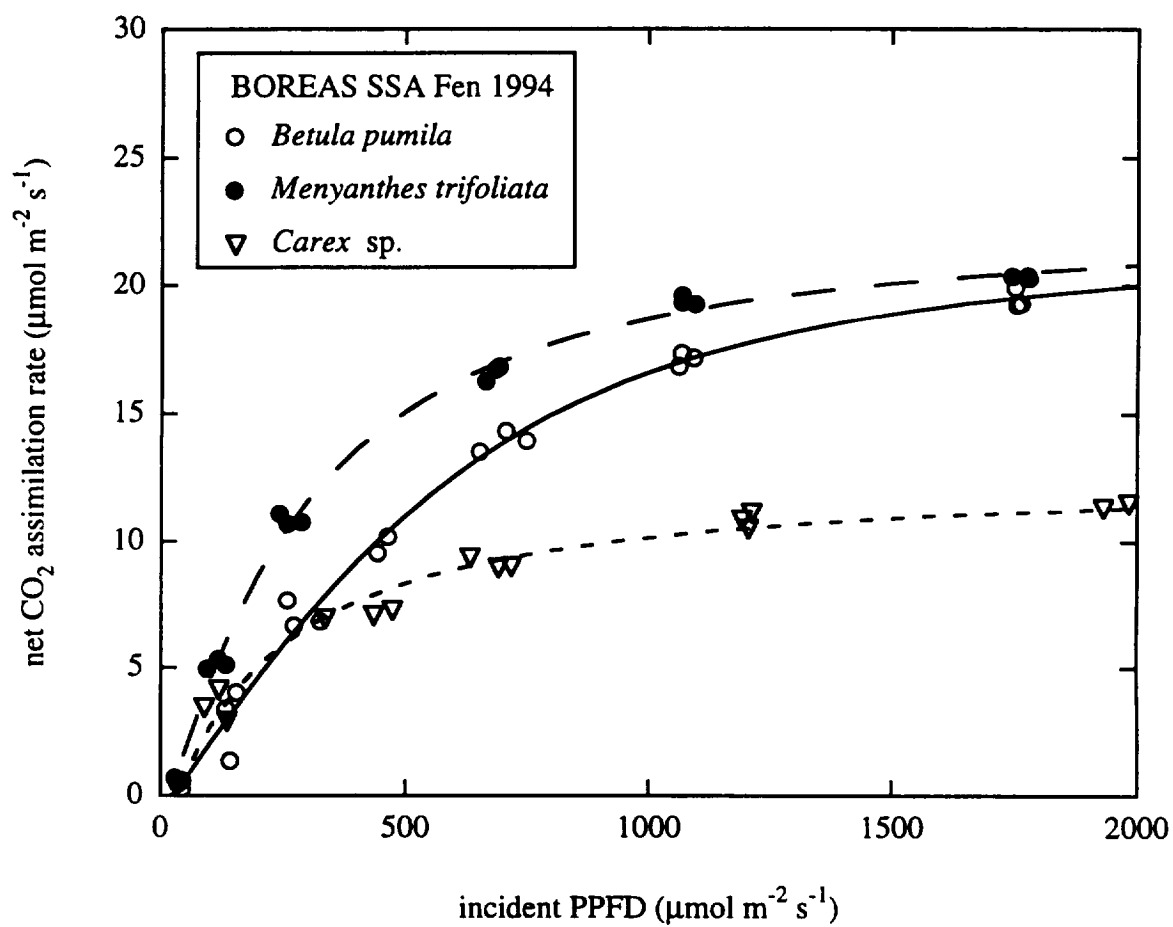


Figure 14. Net CO₂ exchange rate as a function of incident light intensity for the three dominant species at the BOREAS SSA-Fen site.

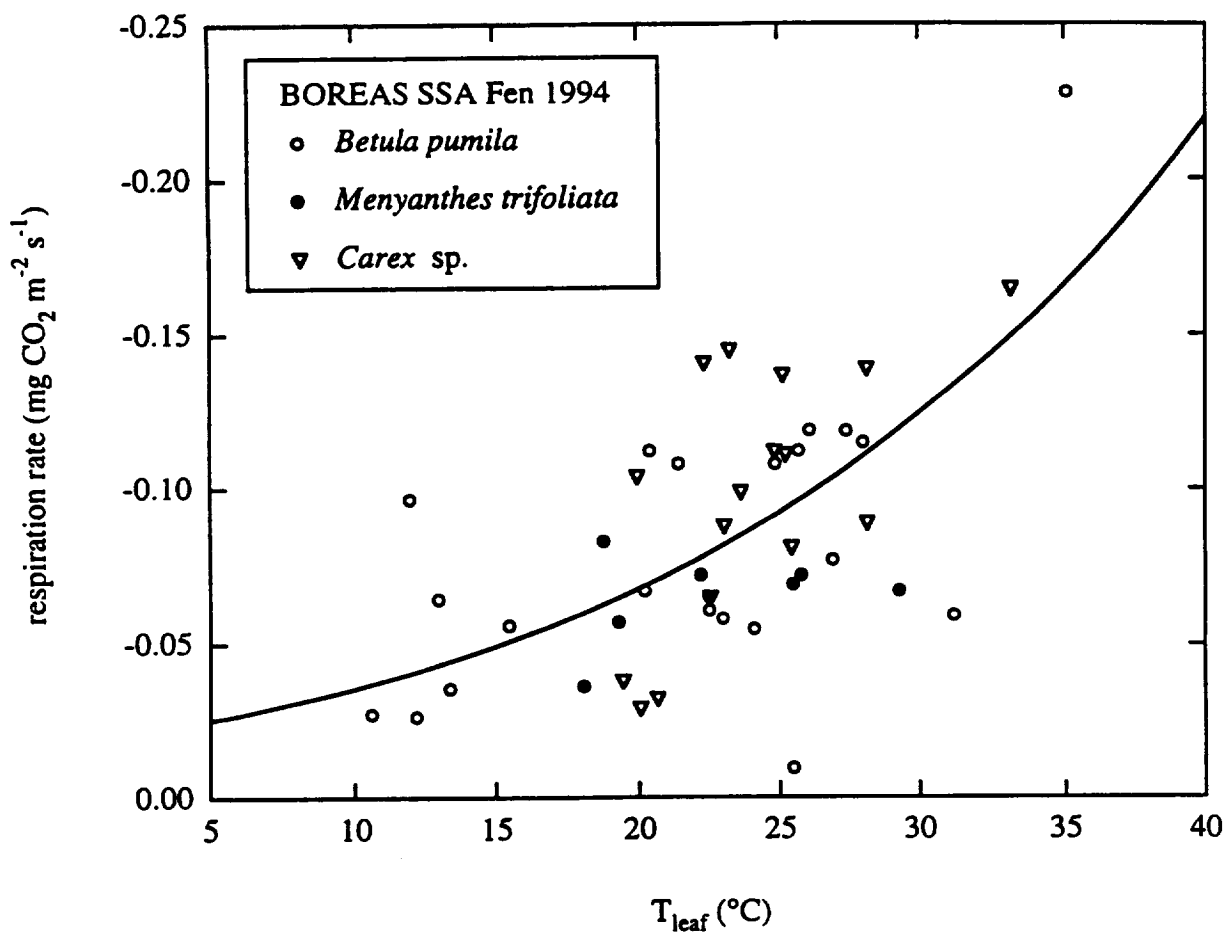


Figure 15.

Relationship between dark respiration rates and leaf temperature for the three dominant species at the BOREAS SSA-Fen site. An exponential curve was fit to all the data points. See text (Sec 3.3) for equation parameters.

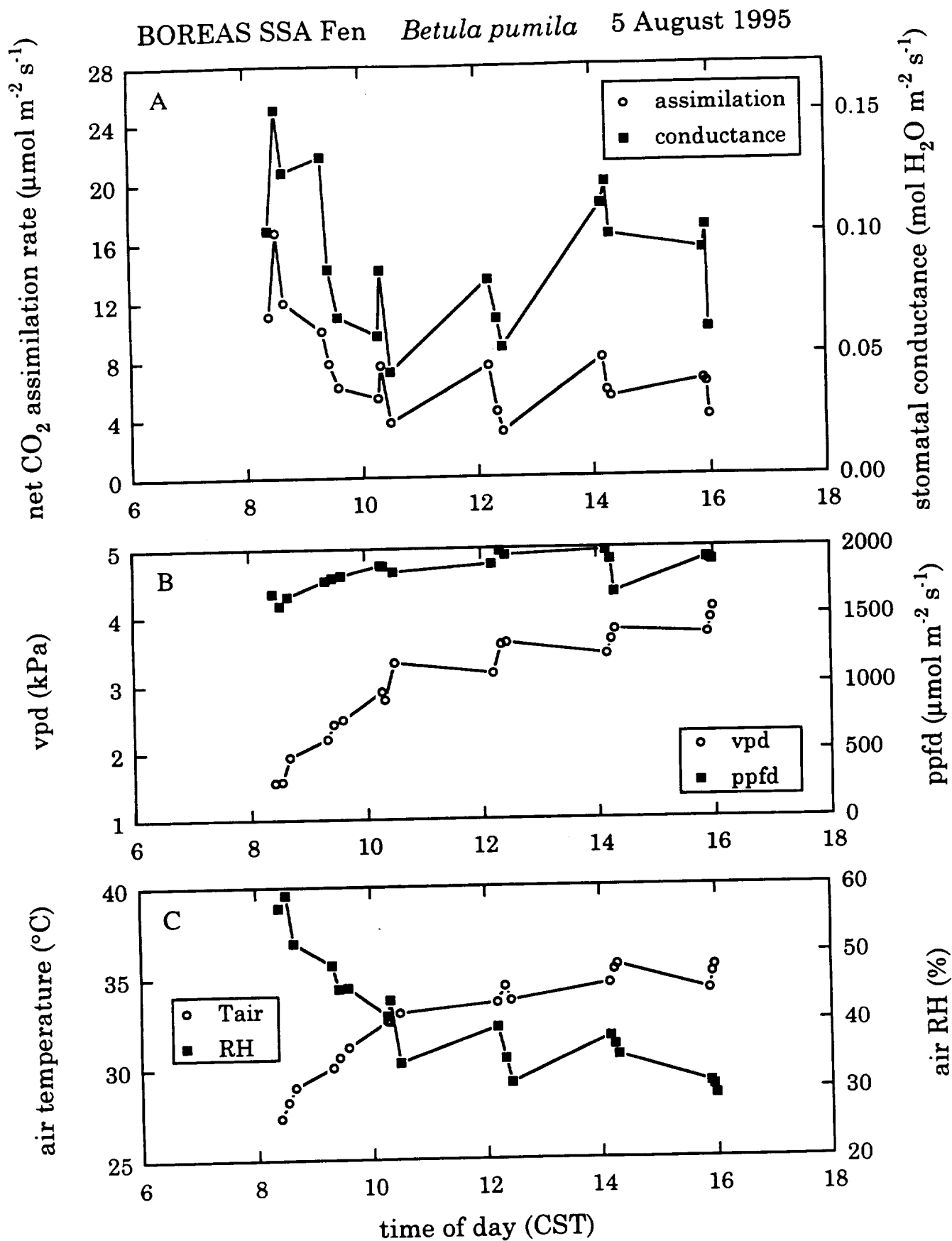


Figure 16. Diurnal course of (A) net CO₂ assimilation rate and stomatal conductance, (B) vpd and ppfd and (C) air temperature and RH for *Betula pumila* at the BOREAS SSA-Fen site on Aug. 5, 1995.

BOREAS SSA Fen- August 14-15, 1995

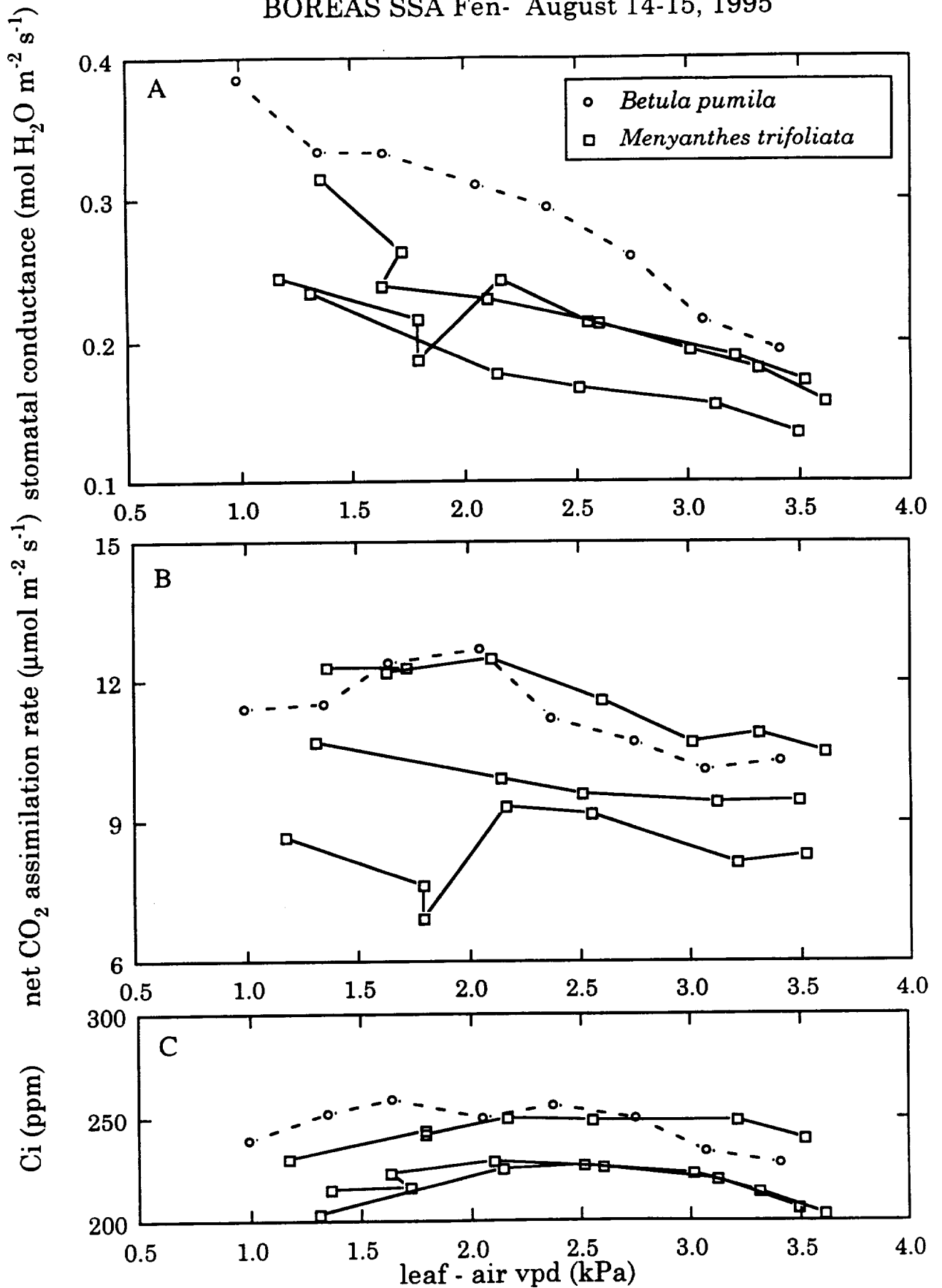


Figure 17. Relationship between stomatal conductance and leaf-air VPD for *Betula pumila* and *Menyanthes trifoliata* at the BOREAS SSA-Fen site.

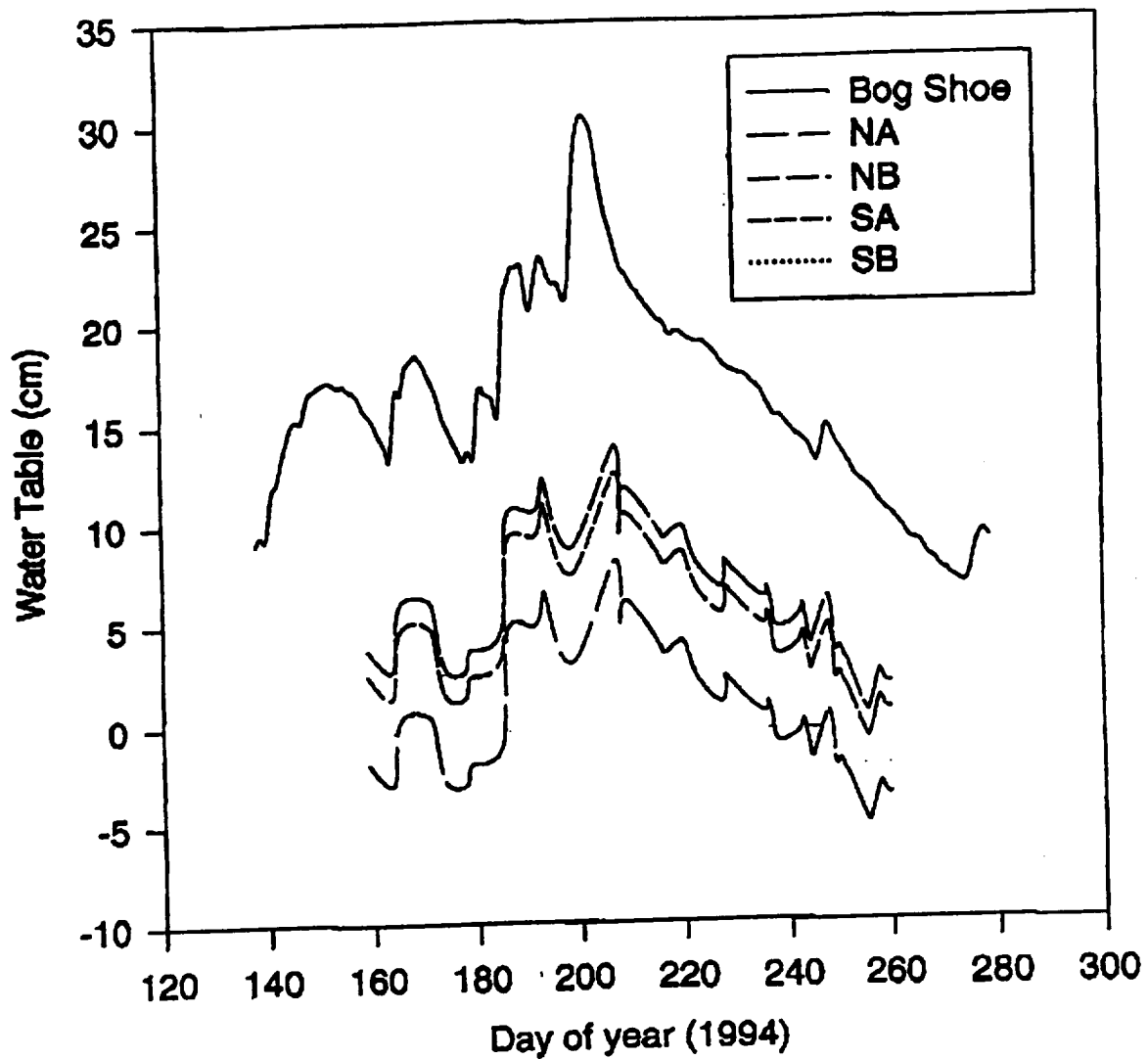


Fig. 18. Water table fluctuations manually recorded from bog wells located at each platform, relative to mean peat surface. Each of the four platforms is identified by a two-letter code indicating the transect (North or South) and the location (A or B) along the transect. The water table profiles for NB and SB were identical. The synthetic hydrograph for each platform is highly correlated ($r=0.96$) to the continuously recorded water table well data, here presented relative to the hollow surface.

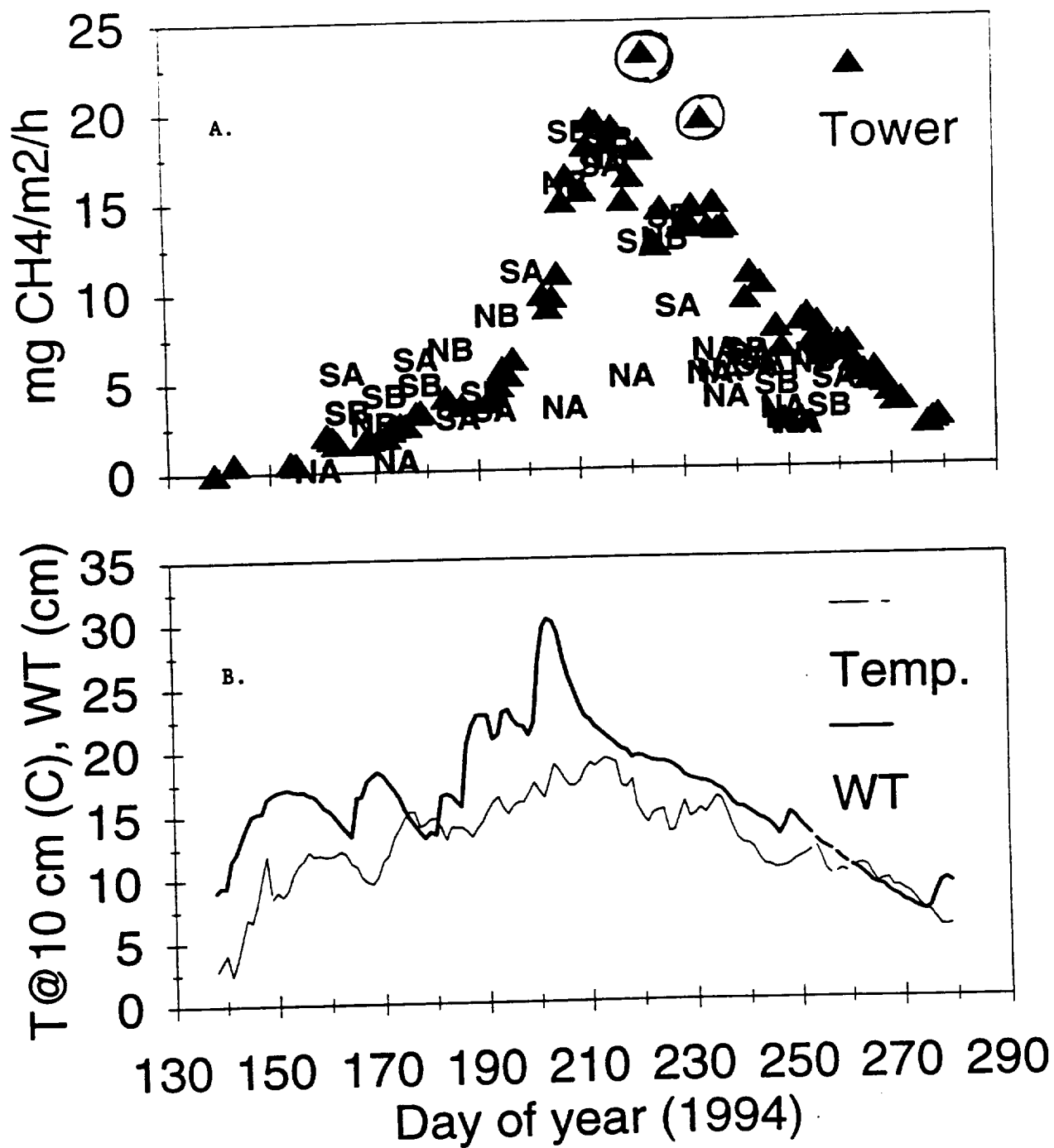


Fig. 19. (A) Time course of CH_4 emissions during the 1994 field campaign. Eddy correlation data are shown as solid triangles, static chamber data are represented by their 2-letter platform code (see caption for Fig. 18). (b) continuously recorded temperature and water table fluctuations.

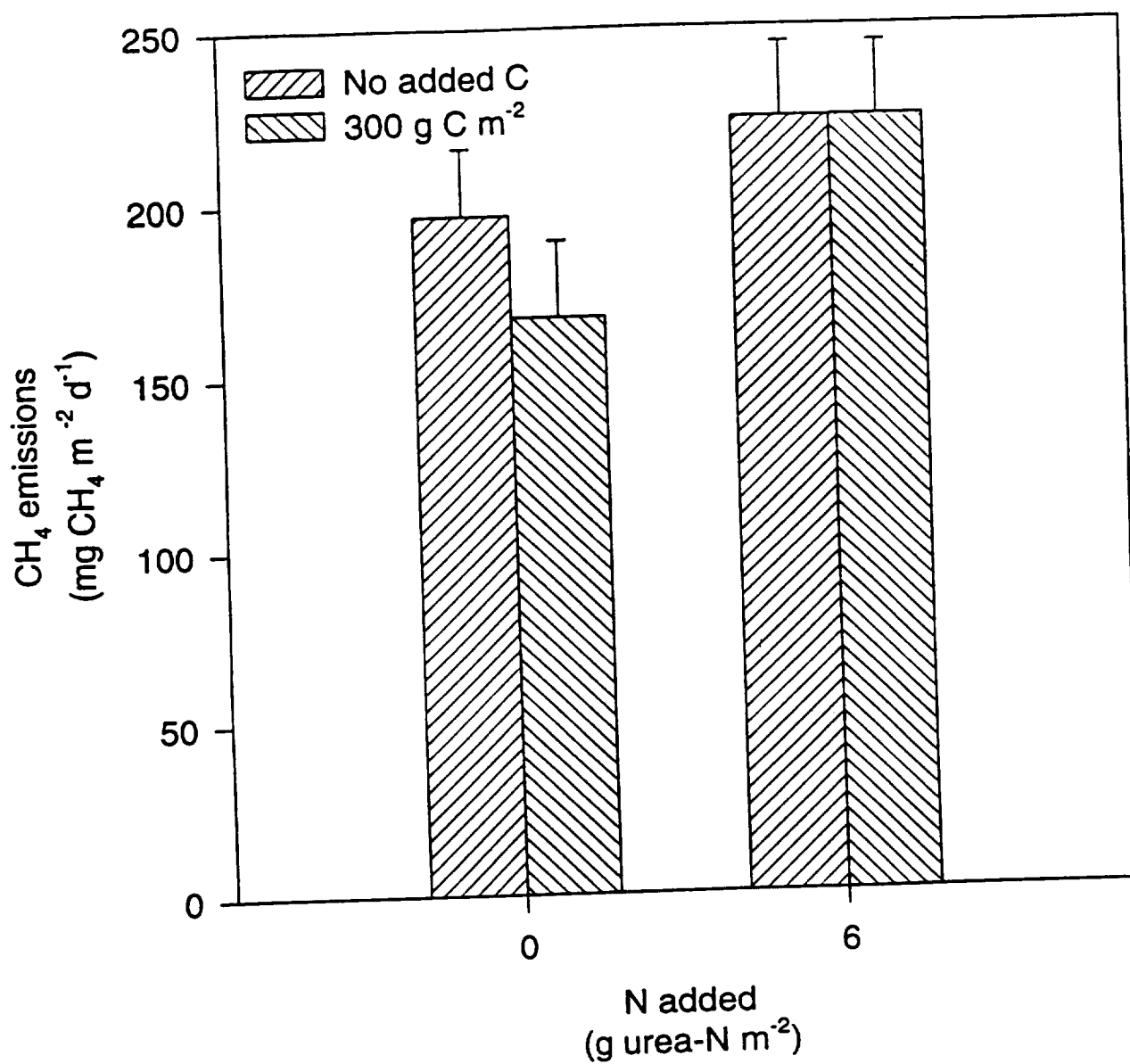


Fig. 20. Response of CH₄ efflux to N and C addition. Error bars are standard errors of the mean.

